

LIGHT CLUSTER FORMATION IN LOW DENSITY
NUCLEAR MATTER AND THE STABILITY OF HOT NUCLEI

تكون الأنوية الخفيفة في المادة النووية قليلة الكثافة وتأثيرها على استقرار
الأنوية الثقيلة الساخنة

By

SAEDA AHMAD YOUSEF AL.TALAHMEH

January 11, 2012

Thesis committee: Prof. Henry Jaqaman (Principal advisor)

Dr. Wafaa Khater (Member)

Dr. Abdallah Sayyed-Ahmad (Member)

This Thesis was submitted in partial fulfillment of the requirements for
the Master's Degree in Physics from the Faculty of Graduate Studies at
Birzeit University, Palestine

LIGHT CLUSTER FORMATION IN LOW DENSITY NUCLEAR
MATTER AND THE STABILITY OF HOT NUCLEI

By

SAEDA AHMAD YOUSEF AL.TALAHMEH

Accepted by the Faculty of Graduate Studies, Birzeit University, in partial fulfillment of the requirements of the degree of Master of Physics

Thesis committee:

Henry Jaqaman Ph.D. (Principal advisor)

Wafaa Khater Ph.D. (Member)

Abdallah Sayyed-Ahmad Ph.D. (Member)

January 11, 2012

ACKNOWLEDGEMENT

I extend sincere thanks and appreciation to Prof. Henry Jaqaman for his continuous support and assistance from the outset until the final steps in this thesis. I would like also to thank the members of my advisory committee, Dr. Abdallah Sayyed-Ahmad and Dr. Wafaa Khater. I'm also thankful to Dr. Wael Qara'een and Dr. Edward Sader and all faculty members at the Department of physics. My thanks and heartfelt appreciations also go to my family and friends.

الإهداء

إلى ربي وهو أجل وأعظم

إلى الإسلام العظيم.

إلى قدوتنا رسول الله محمد صلى الله عليه وسلم.

إلى الذين ضحوا بأرواحهم لتسعد أرواحنا... إلى كل الشهداء.

إلى كل الصامدين وراء قضبان الحديد... إلى الأسرى.

إلى العيون التي ترافقتي دائما... إلى أمي وأبي وكل عائلتي.

إلى النور الذي أهداني إياه الله. إلى نصفي الآخر... إلى عمر.

إلى كل من علمني حرفا.

ABSTRACT

Nuclear matter at low density and finite temperatures consists not only of nucleons but also of clusters of nucleons. In this work we study the problem of hot charged nuclei immersed in a clustered vapor. These nuclei are treated as hot liquid drops that exist in mechanical, thermal, and chemical equilibrium with the surrounding vapor. The effect of inclusion of clusters in the vapor on the limiting temperature and on the instability of hot nuclei is investigated. It was found that the existence of clusters in the vapor lowers the limiting temperature by several MeVs.

ملخص

ان المادة النووية قليلة الكثافة والموجودة في درجات حرارة منخفضة لا تتكون من النيوكليونات فقط ولكن تحتوي ايضا على الأنوية الخفيفة. نقدم في هذا البحث دراسة جديدة نقوم فيها بالتحقق من مدى تأثير هذه الأنوية الخفيفة على استقرار بعض الأنوية الثقيلة الساخنة والمشحونة اذا افترضنا أنها موجودة في حالة اتزان حراري وكيميائي وميكانيكي مع البخار المحيط المحتوي على هذه الأنوية الخفيفة. توصلنا في هذه الدراسة الى أن وجود الأنوية الخفيفة في البخار المحيط يعمل على زيادة عدم استقرار الأنوية الثقيلة المشحونة فتتفكك وتتلاشى على درجات حرارة أكثر انخفاضا لتصبح جزءا من الوسط المحيط.

TABLE OF CONTENTS

Acknowledgement.....	i
الإهداء.....	ii
Abstract.....	iii
الملخص.....	iv
Table of contents.....	v
List of Figures.....	vii
List of Tables.....	x
1. Introduction.....	1
2. Equation of State of ideal quantum gases.....	5
2.1 Ideal Fermi gas Equation of State.....	5
2.2 Infinite system of non-interacting fermions.....	11
2.3 Ideal Bose gas Equation of State.....	17
2.4 Infinite system of non-interacting boson.....	19
3. The Skyrme interaction and the nuclear equation of state.....	21
3.1 The Skyrme interaction.....	21
3.2 Equation of State of a system in the nucleonic model.....	30
3.3 Nuclear Equation of State for asymmetric nuclear matter.....	37

4. Nuclear Statistical Equilibrium (NSE) model	41
4.1 Review of the Equation of State of clustered nuclear matter in various models.....	41
4.2 The Nuclear Statistical Equilibrium (NSE) Model.....	44
4.3 Equation of State of clustered nuclear matter in the NSE model.....	50
5. The Hot Liquid Drop Model and the limiting temperature.....	53
5.1 The Hot Liquid Drop model.....	53
5.2 The coexistence equations.....	58
5.3 The Limiting Temperature.....	60
5.4 Evaluating the vapor asymmetry parameter.....	62
6. Results and Conclusions.....	68
6.1 The coexistence equations with clusters in the vapor.....	68
6.2 The Limiting Temperature.....	70
6.3 Conclusions.....	74
References.....	76
Appendix A.....	78

LIST OF FIGURES

Figure 2.1: Chemical potential of an ideal system of nucleons.....	13
Figure 2.2: Pressure versus density of an ideal Fermi gas.....	14
Figure 2.3: Pressure versus density of an infinite ideal system of nucleons at $T=3\text{MeV}$ and different n	15
Figure 2.4: Pressure versus density of an infinite ideal system of nucleons at $T=6\text{MeV}$ and different n	16
Figure 2.5: Measuring the degeneracy of an infinite ideal system of nucleons.....	17
Figure 2.6: Pressure versus density of an ideal system of alpha nuclei.....	20
Figure 3.1: Binding Energy per nucleon versus mass number A (with pairing energy included).....	27
Figure 3.2: Binding energy per nucleon versus mass number A (without the pairing energy).....	28
Figure 3.3: Experimental results of the binding energy per nucleon.....	28
Figure 3.4: The pressure isotherms of a system of nucleons in the nucleonic model.....	33
Figure 3.5: The chemical potential isotherms of the system of nucleons in the nucleonic model.....	34

Figure 3.6: Finding the critical point when $\sigma=0.25$ from the chemical potential isotherms.....	35
Figure 3.7: Finding the critical point when $\sigma=0.25$ from the pressure isotherms.....	35
Figure 3.8: The effect of different Skyrme parameterizations on the equation of state.....	37
Figure 4.1: Fraction of nucleons in clusters versus total density at $T=4\text{MeV}$	49
Figure 4.2: Fractions of nucleons in clusters versus total density at $T=2\text{MeV}$	50
Figure 4.3: The equation of state of nuclear matter in three different models (the nucleonic model, NSE model, and the ideal model).....	51
Figure 5.1: The vapor, bulk, and drop isotherms at $T=5\text{MeV}$ and $\sigma=0.25$ for the nucleus $^{109}_{47}\text{Ag}$	57
Figure 5.2: The vapor, bulk, and drop isotherms at $T=5\text{MeV}$ and $\sigma=0.25$ for the nucleus $^{208}_{82}\text{Pb}$	58
Figure 5.3: The bulk and drop pressure versus chemical potential curves at $T=5\text{MeV}$, and $\sigma=0.25$ for $^{109}_{47}\text{Ag}$ with the asymmetry terms added only to the drop equations.....	62

Figure 5.4: Determining the limiting temperature for $^{109}_{47}\text{Ag}$ nucleus at $\sigma=0.25$ when the clusters are not included in the vapor.....	63
Figure 5.5: The left hand side of Eq. (5.11.c) versus density of liquid at $T=5\text{MeV}$	64
Figure 5.6: μ_1 versus α_v	65
Figure 6.1: The pressure versus chemical potential curves for the drop and clustered vapor at $T=2.8\text{MeV}$	71
Figure 6.2: Determining the limiting temperature of the hot $^{109}_{47}\text{Ag}$ nucleus in the presence of clusters in the vapor state.....	73

LIST OF TABLES

Table 1: Numerical values of the b coefficients calculated for the ideal Fermi gas	12
Table 2: Parameters of the Skyrme force.....	24
Table 3: The critical values at different Skyrme Parameterizations.....	36
Table 4: Binding energies, masses, and spin degeneracy factors of some light clusters.....	46
Table 5: The Mott densities $\rho_M(0)$ for various clusters at typical temperatures	46
Table 6: The values of the limiting temperatures T_l , and ρ_v , and ρ_l obtained at the limiting temperatures when the asymmetry terms added only to the drop equations	65
Table 7: The values of the limiting temperatures T_l , and ρ_v , and ρ_l obtained at the limiting temperatures when the coexistence equations solved exactly	66
Table 8: Comparison between the results with and without clusters included in the vapor when the vapor asymmetry parameters are neglected	72

CHAPTER 1. INTRODUCTION

Occurrence of the liquid gas phase transition in hot nuclear matter produced in intermediate heavy ion collisions is still the subject of many investigations [1, 2]. A related concept to the liquid gas phase transition is the critical temperature above which only the vapor phase can exist. Below this temperature, the nuclear matter exists in two distinct phases; one is the liquid dense phase that exists inside the nuclei, and the other is the outside vapor dilute gaseous phase in which the nuclei are embedded [1].

Above the critical temperature no liquid state can exist. A theoretical evidence of such possible liquid gas coexistence appears in the behavior of the pressure-density isotherms which are similar to those of the Van der Waals equation of state.

Here we are investigating the thermodynamic stability of hot nuclei embedded in nuclear vapor undergoing a liquid gas phase transition. The finite size of the nuclei reduces their critical temperature when compared with that of infinite nuclear matter [1, 2].

Levit and Bonche [3] demonstrated that uncharged nuclei decay by evaporation of particles while they are heated up to the critical temperature. In contrast, they also showed that charged nuclei are not stable and fragment into parts at a temperature much lower than the critical temperature. This motivated them to introduce the concept of the limiting temperature above which a hot nucleus will fragment into parts and cannot exist in equilibrium with the surrounding vapor. This phenomenon is referred to as the Coulomb instability of hot nuclei. These findings suggest that there is a strong relationship between the Coulomb instability of hot nuclei and the limiting temperature

on the one hand, and the liquid gas phase transition and the critical temperature on the other hand

Studies on the Coulomb instability of hot nucleus [3-8] emphasized that the limiting temperature depends on its surface tension and on the properties of the nuclear matter surrounding it.

Levit and Bonche [3] studied the Coulomb instability of hot nuclei approaching liquid gas phase transition using an equation of state of nuclear matter derived on the basis of the Hartree-Fock approximation with an effective nucleon-nucleon interaction of the Skyrme type. This equation of state included only the first order degeneracy correction. They calculated the limiting temperature and demonstrated that this temperature depends strongly on the properties of the nuclear matter contained in its equation of state, and also on the surface tension of the nuclei.

The work of Levit and Bonche is then extended by Jaqaman [5] who calculated the limiting temperature and showed that in order to have a better estimate of the limiting temperature the asymmetry of the nuclear matter must be taken into account. In another study [7], Jaqaman modified his previous model [5], by introducing a density dependent effective mass and including the effects of the electric charge of the vapor assuming that both the vapor and the drop have uniform charge density. He concluded that including such effects changes the limiting temperature to a value higher than the value obtained by assuming the vapor to be uncharged.

Song and Su [4] studied the Coulomb instability of hot nuclei with the Skyrme interaction. They used the nuclear matter equation of state derived using the finite

temperature real time Green's function method with the mean field approach and nucleon - nucleon interactions of the Skyrme type. They showed that the limiting temperature decreases as the mass number of the nucleus increases. This result was obtained previously by Jaqaman in [5] and later in [8] where the Coulomb instability was studied based on the relativistic mean field approach with derivative scalar coupling.

Coulomb instability [6] was also studied using the mean field theory of Quantum Hadrodynamics (QHD) [6] which describes the nuclear many body problem as a relativistic system of baryons and mesons based on a local Lorentz – invariant Lagrangian density. It was shown that the nuclei described by the QHD model are more stable than that described by the non-relativistic theories where the limiting temperature calculated in the QHD study was larger.

Several studies [9-13] showed that nuclear matter at densities much less than the saturation density tends to form clusters to minimize its energy and entropy. Studies [10, 13] showed that light clusters with mass numbers $A= 2, 3$ and 4 are dominant at low density nuclear matter and so they must be included in any equation of state that describes the nuclear matter at this limit.

In this study we are extending the approach of [5] to the study of Coulomb instability of hot nuclei by including light clusters in the vapor phase and calculating the limiting temperature. Including clusters in the vapor is the main difference between this study and all other studies that investigated the problem of instability of hot nuclei.

This thesis is organized as follows: in chapter (2) the equation of state of ideal quantum gases is discussed, in chapter (3) the Skyrme interaction which is the type of

interaction we assume between nucleons is discussed and the nuclear equation of state is derived. The Nuclear Statistical equilibrium (NSE) model which will be used to derive the equation of state of clustered nuclear matter at low density is the subject of chapter (4), while the hot liquid drop model which is adopted here to describe the hot nucleus is described in chapter (5). In chapter (6) the new results of our study involving the clustered vapor are discussed and our conclusions are presented.

CHAPTER 2. EQUATION OF STATE OF IDEAL QUANTUM GASES

The ideal quantum gas can be defined as a system of non-interacting indistinguishable particles which obey Fermi-Dirac or Bose-Einstein statistics. The equation of state of a system is a mathematical relation in which all the thermodynamic information about the system is encoded. The equation of state connects the main variables of the system (pressure, volume, and temperature) and can be written as:

$$F(P, V, T) = 0$$

In this chapter we will derive two equations of state: one describes the ideal Fermi gas, and the other describes the ideal Bose gas.

2.1. IDEAL FERMI GAS EQUATION OF STATE

The ideal Fermi gas is a quantum mechanical physical system that consists of a large number of non-interacting identical fermions. Fermions are particles that have half integer spin and obey Fermi-Dirac statistics. They are subjected to the Pauli Exclusion Principle which prevents two fermions with the same quantum numbers from existing at the same quantum state.

Protons and neutrons both have a spin of $\frac{1}{2}$, they are fermions, their masses ≈ 940 MeV/c² ($\approx 1.8 \times 10^{-27}$ kg). The main difference between the two particles is the electromagnetic properties of the protons which arise from the positive charge they carry. So, neglecting the electromagnetic properties of protons by switching off the Coulomb interaction between protons enables us to treat protons and neutrons in the same way.

Then we say protons and neutrons are two degenerate states of the same particle called the nucleon. A system of nucleons at low densities can be treated as an ideal Fermi gas.

Other fermions that we will encounter in this thesis are helions and tritons, both are clusters of nucleons, helion clusters are the nuclei of ${}^3\text{He}$ and consist of 2 protons and 1 neutron while the triton clusters are the nuclei of ${}^3\text{H}$ and consist of 2 neutrons and 1 proton.

To derive the equation of state for Fermi systems we will use the Fermi-Dirac Statistics. Consider a system consists of A fermions with single particle energies labeled as: $\varepsilon_1, \varepsilon_2, \dots, \varepsilon_k$. Begin with the Fermi-Dirac distribution function n_i which gives the probability that a certain energy level is occupied at temperature T :

$$\frac{A}{g} = \sum_i n_i = \sum_i \frac{1}{\exp(\beta(\varepsilon_i - \mu)) + 1} \quad (2.1)$$

where: μ is the chemical potential which varies with temperature T and density ρ as we will show later in this chapter, $(\varepsilon_i - \mu)$ is a positive quantity, $\beta = 1/k_b T$, T is the temperature, and k_b is Boltzmann constant. The quantities $k_b T$ and μ are in energy units.

$$k_b = 8.617 \times 10^{-11} \text{ (MeV/K)}$$

We can express the temperature $k_b T = 1 \text{ MeV}$ in energy units as $T = (1.1 \times 10^{10} \text{ K})$ in SI units.

The weight factor g arises from the internal structure of the particles such as spin. For nucleons, $g = 4$ is called the spin-isospin degeneracy factor.

At high temperatures the Fermi system is said to be partially degenerate $[(\varepsilon_i - \mu) \ll k_b T]$ and hence the occupation probability n_i is much smaller than unity.

Recalling that

$$\frac{1}{1+x} = \sum_{n=0}^{\infty} (-1)^n x^n \quad \text{where } |x| < 1, \quad (2.2)$$

we can write

$$\frac{1}{\exp(\beta(\varepsilon_i - \mu)) + 1} = - \sum_{n=1}^{\infty} (-1)^n \exp(-n\beta(\varepsilon_i - \mu)) \quad (2.3)$$

Now we rewrite Eq. (2.1) as:

$$\sum_i \frac{1}{\exp(\beta(\varepsilon_i - \mu)) + 1} = \sum_i [- \sum_{n=1}^{\infty} (-1)^n \exp(-n\beta(\varepsilon_i - \mu))] \quad (2.4)$$

For simplification we use:

$$Q(\beta) = \sum_i e^{-\beta\varepsilon_i} \quad (2.5)$$

where $Q(\beta)$ is a dimensionless quantity and it is called the classical canonical partition function.

We use $z = e^{\beta\mu}$, where z is the fugacity of the system. Fugacity is a dimensionless quantity that is related to the thermodynamical activity of the system which measures the effective concentration of a species in a mixture, the fugacity we deal with in this study represents the absolute activity. Using these abbreviations we rewrite Eq. (2.4) as:

$$\frac{A}{g} = Q(\beta)z - Q(2\beta)z^2 + Q(3\beta)z^3 - \dots \quad (2.6)$$

Dividing Eq. (2.6) by $Q(\beta)$ and using the abbreviation $\frac{Q(n\beta)}{Q(\beta)} = S_n(\beta)$

we get

$$\eta = \frac{A}{gQ(\beta)} = z - S_2(\beta)z^2 + S_3(\beta)z^3 - \dots \quad (2.7)$$

where η is a measure of the degeneracy of the gas.

We see in Eq. (2.7) that η is a power series in z and can be written as:

$$\eta = \sum_i c_i z^i \quad (2.8)$$

The series in Eq. (2.8) can be inverted to get z as a power series in η that is to write z in the form:

$$z = \sum_i a_i \eta^i. \quad (2.9)$$

This can be done using series reversion as explained in Appendix A.

Using this method of series reversion the coefficients of the series in Eq. (2.9) were calculated as follows:

$$a_1 = 1$$

$$a_2 = S_2(\beta)$$

$$a_3 = 2S_2^2(\beta) - S_3(\beta)$$

$$a_4 = -5S_2(\beta)S_3(\beta) + S_4(\beta) + 5S_2^3(\beta) \quad (2.10)$$

$$a_5 = 6S_2(\beta)S_4(\beta) + 3S_3^2(\beta) + 14S_2^4(\beta) - S_5(\beta) - 21S_2^2(\beta)S_3(\beta)$$

$$a_6 = -7S_2(\beta)S_5(\beta) - 7S_3(\beta)S_4(\beta) - 84S_2^3(\beta)S_3(\beta) + S_6(\beta) + 28S_2(\beta)S_3^2(\beta) + 42S_2^5(\beta) + 28S_2^2(\beta)S_4(\beta)$$

$$a_7 =$$

$$8S_2(\beta)S_6(\beta) + 8S_3(\beta)S_5(\beta) + 4S_4^2(\beta) + 120S_2^3(\beta)S_4(\beta) + 180S_2^2(\beta)S_3^2(\beta) + 132S_2^6(\beta) - S_7(\beta) - 36S_2^2(\beta)S_5(\beta) - 72S_2(\beta)S_3(\beta)S_4(\beta) - 12S_3^3(\beta) - 330S_2^4(\beta)S_3(\beta)$$

Recalling that $z = e^{\beta\mu}$ we get,

$$\mu = k_b T \ln(z) = k_b T \ln\left(\sum_{i=1}^{\infty} a_i \eta^i\right) \quad (2.11)$$

$$= k_b T \ln(\eta) + k_b T \ln\left(1 + \sum_{i=2}^{\infty} a_i \eta^{i-1}\right) \quad (2.12)$$

Consider the second term in Eq. (2.12):

$$k_b T \ln\left(1 + \sum_{i=2}^{\infty} a_i \eta^{i-1}\right) = k_b T \ln(1 + \delta) \quad (2.13)$$

where

$$\delta = \sum_{i=2}^{\infty} a_i \eta^{i-1} \quad (2.14)$$

We use the expansion:

$$\ln(1 + \delta) = \delta - \frac{\delta^2}{2} + \frac{\delta^3}{3} - \frac{\delta^4}{4} + \frac{\delta^5}{5} - \frac{\delta^6}{6} + \dots \quad (2.15)$$

We use the definition of δ as defined in Eq. (2.14), and rewrite the second term of Eq.

(2.12) as:

$$\begin{aligned}
\ln(1 + \delta) &= a_2\eta + \left(a_3 - \frac{a_2^2}{2}\right)\eta^2 + \left(a_4 - \frac{a_2^3}{2} - a_2a_3\right)\eta^3 \\
&+ \left(a_5 - \frac{a_2^4}{2} - a_2a_4 + a_2^2a_3 - \frac{a_2^4}{4}\right)\eta^4 \\
&+ \left(a_6 - a_2a_5 - a_3a_4 + a_2a_3^2 + a_2^2a_4 - a_2^3a_3 + \frac{a_2^5}{5}\right)\eta^5 \\
&+ \left(a_7 - a_2a_6 - a_3a_5 - \frac{a_2^4}{2} + a_2^2a_5 + 2a_2a_3a_4 + \frac{a_2^3}{3} - \frac{3}{2}a_2^2a_3^2 \right. \\
&\quad \left. - a_2^3a_4 + a_2^4a_3 - \frac{a_2^6}{6}\right)\eta^6 + \dots
\end{aligned} \tag{2.16}$$

We can rewrite Eq. (2.12) as:

$$\mu = k_b T \ln(\eta) + k_b T \sum_{i=1}^{\infty} b_i \eta^i \tag{2.17}$$

The b coefficients are given in terms of the a coefficients as follows:

$$b_1 = a_2$$

$$b_2 = a_3 - \frac{a_2^2}{2}$$

$$b_3 = a_4 + \frac{a_2^3}{2} - a_2a_3$$

$$b_4 = a_5 - \frac{a_2^4}{2} - a_2a_4 + a_2^2a_3 - \frac{a_2^4}{4} \tag{2.18}$$

$$b_5 = a_6 - a_2a_5 - a_3a_4 + a_2a_3^2 + a_2^2a_4 - a_2^3a_3 + \frac{a_2^5}{5}$$

$$b_6 = a_7 - a_2a_6 - a_3a_5 - \frac{a_2^4}{2} + a_2^2a_5 + 2a_2a_3a_4 + \frac{a_2^3}{3} - \frac{3}{2}a_2^2a_3^2 - a_2^3a_4 + a_2^4a_3 - \frac{a_2^6}{6}$$

So, we finished deriving the equation of state for the ideal Fermi gas which is now given by Eq. (2.17). with the b coefficients given in Eqs. (2.18).

2.2. INFINITE SYSTEM OF NON-INTERACTING FERMIONS

The procedure above is the general case; let us now apply this procedure on an infinite ideal Fermi gas such as the infinite system of non-interacting nucleons which we mentioned previously as an example of fermions, we will consider this system later in this thesis. For such a system the single particle energies are specified and have the values:

$$\varepsilon_k = \frac{\hbar^2 k^2}{2m} \quad (2.19)$$

where m is the mass of the particle, and k is the wave number of the particle. It is related to the wavelength λ through the relation $k = \frac{2\pi}{\lambda}$.

The partition function of an ideal gas of volume V is:

$$Q(\beta) = \frac{V}{\lambda_T^3} \quad (2.20)$$

where $\lambda_T^3 = \left(\frac{2\pi\hbar^2}{mk_bT}\right)^{\frac{3}{2}}$ Is the thermal wavelength of the gas particle which is the mean De Broglie wavelength of the gas particles in an ideal gas evaluated at temperature T .

Now we have:

$$\eta = \frac{A}{gQ(\beta)} = \frac{\lambda_T^3 A}{gV} = \frac{\rho}{g} \lambda_T^3 \quad (2.21)$$

where ρ is the particle number density. Also for an ideal gas:

$$S_n(\beta) = \frac{Q(n\beta)}{Q(\beta)} = n^{-3} \quad (2.22)$$

Using Eqs. (2.21) and (2.22), we rewrite the equation of state in the following form:

$$\mu(T, \rho) = k_b T \left(\ln \left(\frac{\lambda_T^3 \rho}{g} \right) + \sum_{n=1}^{\infty} b_n \left(\frac{\lambda_T^3 \rho}{g} \right)^n \right) \quad (2.23)$$

We use MATLAB to evaluate the b coefficients and our results are listed in Table 1.

	b_n	$\left(\frac{n}{n+1} \right) b_n$
n=1	0.3535533905933	0.1767766952966
n=2	-0.0049500897299	-0.0033000598199
n=3	$1.483857713 \times 10^{-4}$	$1.112893285 \times 10^{-4}$
n=4	$-4.4256301 \times 10^{-6}$	$-3.5405041 \times 10^{-6}$
n=5	1.006362×10^{-7}	8.38635×10^{-8}
n=6	-4.272×10^{-10}	-3.662×10^{-10}

Table 1 Numerical values of the b coefficients calculated for the ideal Fermi gas

The second column is added to simplify the comparison with the results of [5]. In this reference the b coefficients are defined to be the coefficients of the pressure series as will be shown next in Eq. (2.26).

In Figure 2.1 the chemical potential given by Eq. (2.23) is plotted for an infinite system of non-interacting nucleons at three different temperatures. In this case $g=4$ the spin-isospin degeneracy of the nucleon.

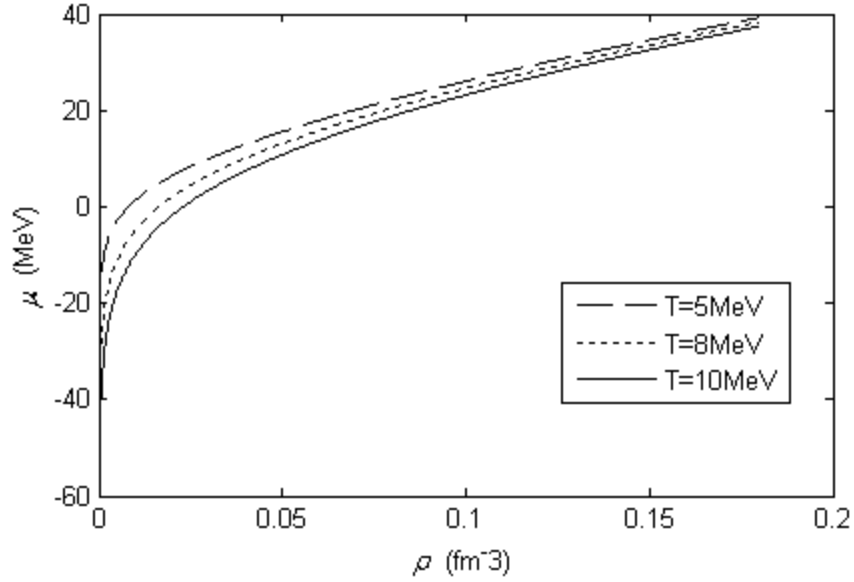


Figure 2.1: Shows the chemical potential of an infinite system of non-interacting nucleons as a function of density at three different temperatures.

The pressure $P(\rho, T)$ is related to the chemical potential $\mu(\rho, T)$ by:

$$P = \rho\mu - f(\rho, T) \quad (2.24)$$

and

$$\mu = - \left[\frac{\partial f}{\partial \rho} \right]_T \quad (2.25)$$

where

$f = \frac{F}{V}$ is the Helmholtz free energy density of the system.

Using Eqs. (2.24) and (2.25) we rewrite the pressure of the infinite system of non-interacting nucleons in the form:

$$P = k_b T \left(1 + \sum_{n=1}^{\infty} \left[\left(\frac{n}{n+1} b_n \right) \left(\frac{\lambda_T^3 \rho}{g} \right)^n \right] \right) \quad (2.26)$$

where: $\left(\frac{n}{n+1}b_n\right)$ are the coefficients of the pressure given in the last column of Table 1.

The pressure given by Eq. (2.26) can also be used to calculate the pressure of infinite system of non-interacting tritons, and infinite system of non-interacting helions by using $g=2$ instead of using $g=4$ for nucleons.

Figure 2.2 shows the pressure for an infinite system of non-interacting nucleons at three different temperatures.

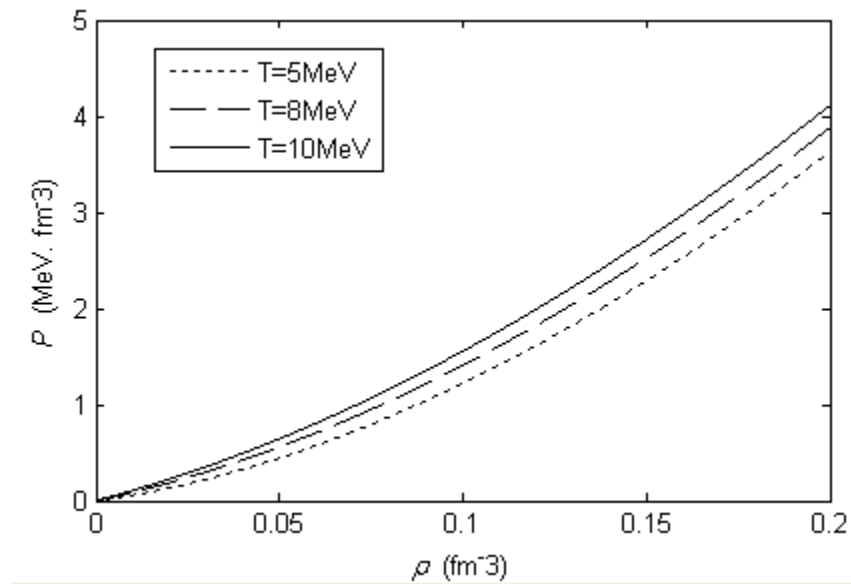


Figure 2.2: Shows pressure versus density of an infinite system of non-interacting nucleons, at three different temperatures

In order to investigate the convergence of the series in Eq. (2.26), the pressure of an infinite system of non-interacting nucleons is plotted in Figure 2.3 below for different orders of degeneracy n .

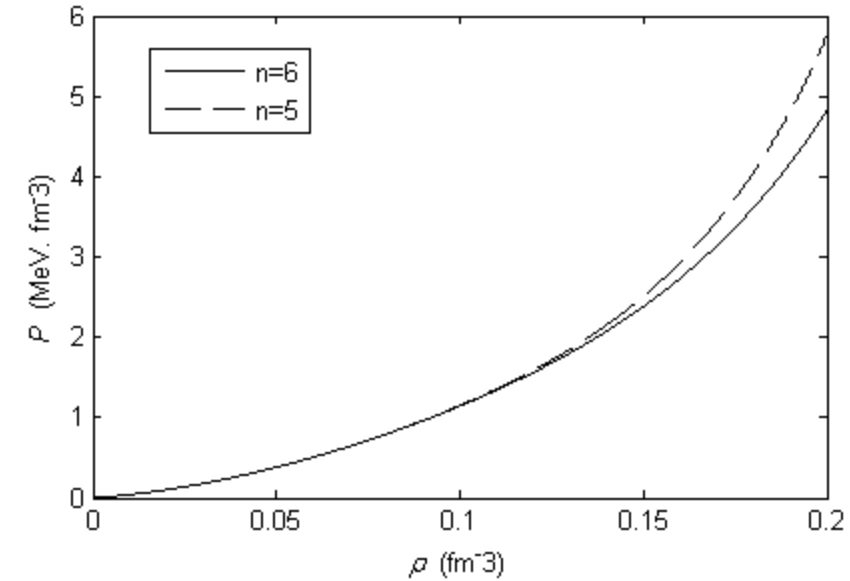


Figure 2.3: Shows pressure versus density of an infinite system of non-interacting nucleons at different n at $T=3\text{MeV}$.

Figure 2.3 shows that the pressure series is convergent at low densities up to about $0.12 \text{ nucleon}/\text{fm}^3$ for $T=3\text{MeV}$.

To investigate the convergence at higher temperatures the pressure of an infinite system of non-interacting nucleons is plotted in Figure 2.4 below for $T=6\text{MeV}$. In Figure 2.4 we note that the pressure series is convergent at densities up to $0.2 \text{ nucleon}/\text{fm}^3$.

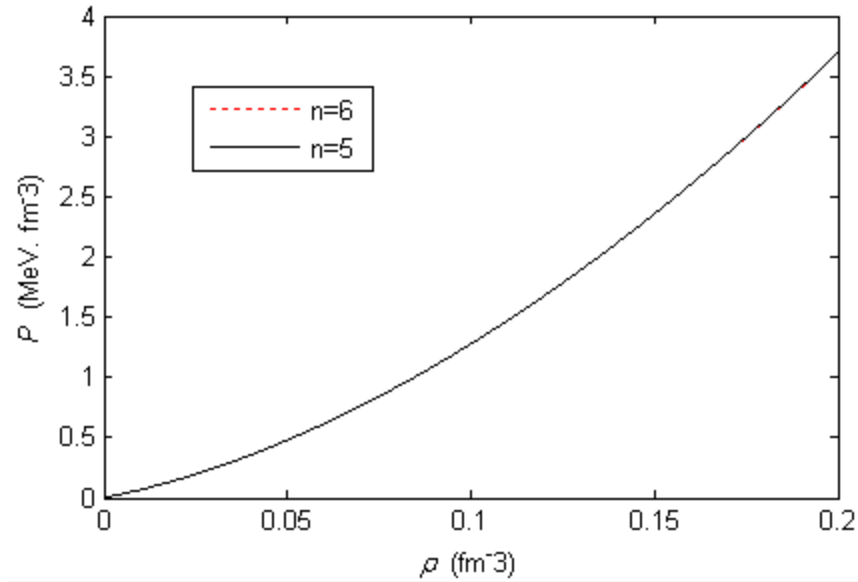


Figure 2.4: Shows the pressure of an infinite system of non-interacting nucleons at $T=6\text{MeV}$

Before we leave the ideal Fermi gas, I will comment on the parameter η that was defined in Eq. (2.7). We mentioned that this parameter is a measure of the degeneracy of the gas. For the ideal Fermi gas the degeneracy represents the number of fermions that have energies less than the Fermi energy (defined as the chemical potential calculated at $T=0\text{K}$) at any temperature T . So, the higher value that the parameter η has at a certain temperature the higher is the degeneracy of the system at that temperature. For an infinite system of non-interacting nucleons we have:

$$\eta = \frac{A}{gQ(\beta)} = \frac{\lambda_T^3 \rho}{g} = \frac{\rho}{4} \lambda_T^3$$

This degeneracy parameter is plotted in Figure 2.5 at three different temperatures.

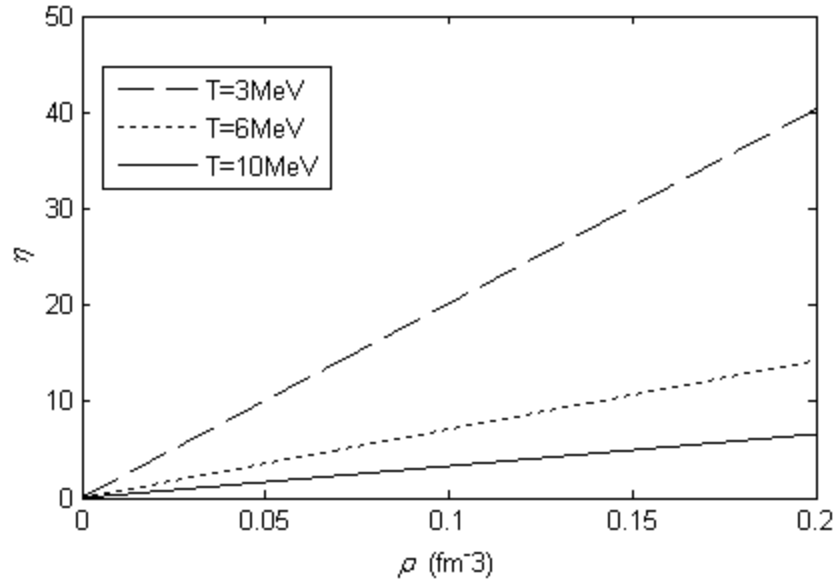


Figure 2.5: Shows how to measure the degeneracy parameter η of an infinite system of non-interacting nucleons at three different temperatures. 3, 6, and 10 MeV

Figure 2.5 shows that the degeneracy increases with lowering the temperature, at $T=3\text{MeV}$ the system is highly degenerate except at low density.

2.3. IDEAL BOSE GAS EQUATION OF STATE

The Ideal Bose gas is a quantum mechanical physical system that consists of a large number of bosons. Bosons are particles that have an integer spin and obey Bose Einstein Statistics. Examples of bosons are alpha particles which consist of 2 protons and 2 neutrons and have spin=0 as well as deuterons which consist of 1 proton and 1 neutron and have spin=1.

In the ideal Bose gas and at low enough temperature all bosons are pushed down to the ground state, this is attributed to the infinite occupancy of the ground state. This phenomenon is called the Bose- Einstein condensation a phenomenon that does not occur in the Fermi systems because of the Pauli Exclusion Principle.

The same procedure used in deriving the equation of state of the ideal Fermi gas above is repeated here to get the equation of state of the ideal Bose gas, starting from the Bose-Einstein distribution function n_i :

$$\frac{A}{g} = \sum_i n_i = \sum_{i=1}^{\infty} \frac{1}{\exp(\beta(\varepsilon_i - \mu)) - 1} \quad (2.27)$$

Following the same lines of the procedure done for the ideal Fermi gas we get for the ideal Bose gas in comparison with Eq. (2.6):

$$\frac{A}{g} = Q(\beta)z + Q(2\beta)z^2 + Q(3\beta)z^3 + \dots \quad (2.28)$$

then

$$\eta = \frac{A}{gQ(\beta)} = z + S_2(\beta)z^2 + S_3(\beta)z^3 + \dots \quad (2.29)$$

In analogy with the Eq. (2.9) for the ideal Fermi gas we now get:

$$z = \sum_i r_i \eta^i \quad (2.30)$$

The r coefficients are calculated following the same way done before for the ideal Fermi gas. We found that these coefficients are related to the a coefficients through the relation:

$$r_n = (-1)^{n+1} a_n \quad (2.31)$$

Also in comparison with Eq. (2.17) derived for the ideal Fermi gas, we have for the ideal Bose gas

$$\mu = k_b T \ln(\eta) + k_b T \sum_{i=1}^{\infty} d_i \eta^i \quad (2.32)$$

where the d_i coefficients are related to the b_i coefficients of the ideal Fermi gas through the relation:

$$d_n = (-1)^n b_n \quad (2.33)$$

Now we obtain the equation of state of the ideal Bose gas which is given by Eq. (2.32).

The d coefficients are given in Eq. (2.33).

2.4. INFINITE SYSTEM OF NON-INTERACTING BOSONS

In analogy with the equation of state derived earlier in section 2.2 for an infinite system of non-interacting fermions we derive in this section the equation of state for an infinite system of non-interacting bosons. The single particle energies for such a system are specified, they are given by:

$$\varepsilon_k = \frac{\hbar^2 k^2}{2m}$$

Following the same lines done in deriving Eq. (2.23) for the infinite system of non-interacting nucleons we obtain for an infinite system of non-interacting bosons:

$$\mu(T, \rho) = k_b T \left(\ln \left(\frac{\lambda_T^3 \rho}{g} \right) + \sum_{n=1}^{\infty} d_n \left(\frac{\lambda_T^3 \rho}{g} \right)^n \right) \quad (2.34)$$

Using Eqs. (2.24) and (2.25) we write the pressure of an infinite ideal system of non-interacting bosons as:

$$P = k_b T \left(1 + \sum_{n=1}^{\infty} \left[\frac{n}{n+1} d_n \right] \left(\frac{\lambda_T^3 \rho}{g} \right)^n \right) \quad (2.35)$$

We mentioned previously that alpha particles are bosons with zero spin. To show the behavior of bosons Eq. (2.35) is plotted in Figure 2.6 for an infinite system of non-

interacting alpha particles at three different temperatures. The fact that the pressure is negative for almost all densities at the lower temperature reflects the approach to Bose-Einstein condensation.

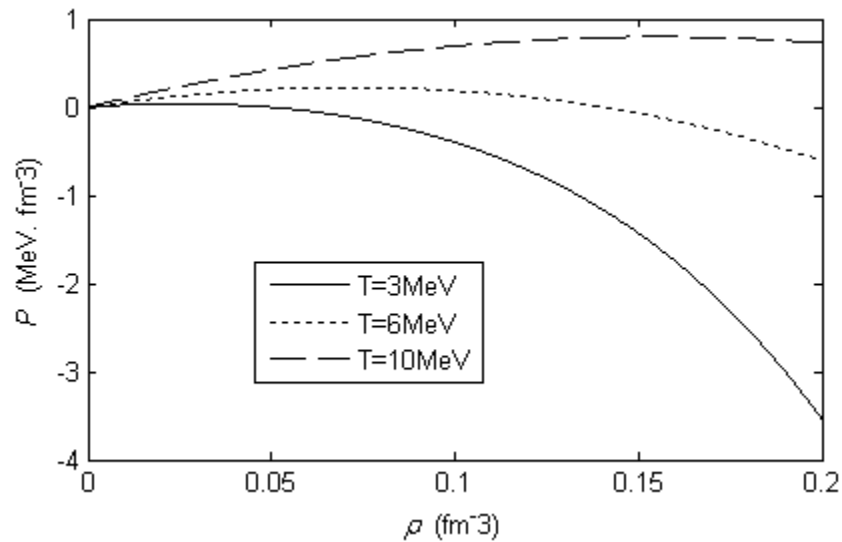


Figure 2.6: shows the pressure of an infinite system of non-interacting alpha particles at three different temperatures 3, 6 and 10 MeV.

The value of the factor g in Eq. (2.35) differs for different bosons, for alpha particles $g = 1$ and for deuterons $g = 3$. We will use Eq. (2.26) and Eq. (2.35) later in chapter (4) when discussing the NSE model to calculate the partial pressures of clusters in clustered nuclear matter.

CHAPTER 3. THE SKYRME INTERACTION AND THE NUCLEAR

EQUATION OF STATE

To describe the interactions between nucleons in nuclear matter many forces were suggested and investigated; one of these forces is the Skyrme interaction which is a zero range interaction whose use simplifies calculations. This interaction is used in [5] and is the type of interaction that we will use in this thesis when we investigate the instability of hot nuclei embedded in a vapor of clustered nuclear matter.

3.1. THE SKYRME INTERACTION

The Skyrme interaction is just an approximation that is used to represent the effective nucleon force and it is only valid at low relative momenta. The original form of this interaction can be written as:

$$V = \sum_{i<j} V_{ij} + \sum_{i<j<k} V_{ijk} \quad (3.1)$$

where:

V_{ij} represents the two body interaction and,

V_{ijk} represents the three body interaction.

Derivations of some nuclear properties using the Skyrme interaction are contained in [14]. In this reference two and three body interactions are included, where it was shown that three body interactions are equivalent to a two body density dependent interaction. This is useful in describing the way in which the interaction between nucleons in nuclear matter is influenced by the presence of other nucleons. The Skyrme

interaction was proposed by Skyrme [15] and used by Vautherin and Brink [14] to reproduce the properties of infinite nuclear matter as well as finite nuclei.

A general form of the Skyrme interaction that was used in [7] is:

$$V_{12} = -t_0(1 + x_0 P_\sigma) \delta(\vec{r}_1 - \vec{r}_2) + \frac{1}{2} t_1 \left[\tilde{P}^2 \delta(\vec{r}_1 - \vec{r}_2) + \delta(\vec{r}_1 - \vec{r}_2) \tilde{P}^2 \right] \quad (3.2)$$

$$+ t_2 \tilde{P} \cdot \delta(\vec{r}_1 - \vec{r}_2) \tilde{P} + \frac{1}{6} t_3 (1 + x_3 P_\sigma) \rho^\sigma \left[\frac{\vec{r}_1 + \vec{r}_2}{2} \right] \delta(\vec{r}_1 - \vec{r}_2)$$

where \vec{r}_1 and \vec{r}_2 are the position vectors of the two nucleons relative to a reference point.

P_σ is the spin exchange operator.

$$\vec{P} = \frac{\vec{v}_1 - \vec{v}_2}{2i} \quad \text{and} \quad \tilde{P} = -\frac{\vec{v}_1 - \vec{v}_2}{2i} \quad \text{are the relative momenta and}$$

x_0, x_3, t_0, t_1, t_2 and t_3 are the Skyrme interaction parameters. These parameters can be determined phenomenologically by fitting the ground state properties of nuclear matter such as the binding energy and the saturation density. The t_1 and t_2 parameters are the finite range terms which reflect the fact that the inter-nucleon force has a finite range and not a zero range as assumed in the simplest Skyrme model. These parameters are velocity dependent, and they lead to an effective mass m^* given by the equation [14]:

$$\frac{\hbar^2}{2m_q^*} = \frac{\hbar^2}{2m_q} + \frac{1}{4} (t_1 + t_2) \rho + \frac{1}{8} (t_2 - t_1) \rho_q$$

where: ρ is the nuclear matter total density, $q=p$ for protons and n for neutrons.

It is seen that if $t_1 = t_2 = 0$, then $m^* = m$.

The parameter σ is used to control the incompressibility of nuclear matter without changing its binding energy. The incompressibility is a measure of the relative volume change of a fluid or solid when pressure is changed. A general definition of the incompressibility is given by:

$$K = -\frac{1}{V} \frac{\partial P}{\partial V}$$

where V is the volume and P is the pressure of the nuclear matter. The minus sign indicates that the incompressibility is always a positive quantity.

For finite nuclear matter another relation for the incompressibility is derived and it is given by:

$$K = R^2 \left(\frac{\partial^2 E}{\partial R^2} \right)_{\rho_0} = 9\rho_0^2 \frac{\partial^2 E}{\partial \rho^2}$$

where $R \sim \rho^{-1/3}$ is the nuclear ground state radius.

In order not to complicate the calculations and since the relative momenta are small we will neglect the momentum dependent terms in Eq. (3.2) that contain the finite range parameters (t_1 and t_2). We now get the zero range Skyrme type force:

$$V_{12} = -t_0(1 + x_0 P_\sigma) \delta(\vec{r}_1 - \vec{r}_2) + \frac{1}{6} t_3 (1 + x_3 P_\sigma) \rho^\sigma \left[\frac{\vec{r}_1 + \vec{r}_2}{2} \right] \delta(\vec{r}_1 - \vec{r}_2) \quad (3.3)$$

This is the form of the Skyrme interaction we are assuming in this thesis. For symmetric nuclear matter in which protons and neutrons are treated in the same manner and no Coulomb force acts between protons, the interaction does not depend on x_0 and x_3 and is given by:

$$V_{12} = -t_0 \delta(\vec{r}_1 - \vec{r}_2) + \frac{1}{6} t_3 \rho^\sigma \left[\frac{\vec{r}_1 + \vec{r}_2}{2} \right] \delta(\vec{r}_1 - \vec{r}_2) \quad (3.4)$$

The Skyrme parameters we used are summarized in Table 2. The parameter x_3 is usually given the value of 1.

	x_0	$a_0 \rho_0$ (MeV)	$a_3 \rho_0^{1+\sigma}$ (MeV)	Critical temperature	Incompressibility (MeV)
$\sigma = 0.25$	0.75	136	96	17.3 MeV	222
$\sigma = 1$	0.47	64	24	22.9 MeV	384

Table 2: parameters of the Skyrme force [5].

The relations that connect the parameters are as follows:

$$a_0 = \frac{3}{8} t_0 \quad (3.5)$$

$$a_3 = \frac{1}{16} t_3 \quad (3.6)$$

$$\sigma = \frac{(K - 9E_B - E_K)}{(9E_B + 3E_K)} \quad (3.7)$$

$$a_0 \rho_0 = \left[(1 + \sigma) E_B + \left(\sigma + \frac{1}{3} \right) E_K \right] / \sigma \quad (3.8)$$

$$a_3 \rho_0^{1+\sigma} = (E_B + E_K/3) / \sigma \quad (3.9)$$

E_B : is the nuclear matter binding energy per particle.

E_K : is the nuclear matter kinetic energy per particle.

K is the nuclear incompressibility. The incompressibility of a nucleus can be calculated from the energy required to excite a nucleus without changing its shape.

ρ_0 is the saturation density or the density of nuclear matter that is distributed uniformly in the interior of a heavy nucleus of large radius. The value of ρ_0 is inferred from the maximum density of finite nuclei, the commonly used value is [1, 3, 5, 7]:

$$\rho_0 = 0.17 fm^{-3}$$

This value differs from the value of the average density of finite nuclei which is approximated as $\rho = \frac{3}{4\pi r_0^3} \approx 0.14 fm^{-3}$ for $r_0 = 1.2 fm$. The difference between these two values is attributed to the absence of the surface region in nuclear matter.

The binding energy per particle of infinite nuclear matter (what is simply called nuclear matter) is derived from the Weizsaecker mass formula for the binding energy of a nucleus containing N neutrons and $Z=A-N$ protons:

$$B(Z, N) = \alpha_1 A - \alpha_2 A^{2/3} - \alpha_3 \frac{Z(Z-1)}{A^{1/3}} - \alpha_4 \frac{(N-Z)^2}{A} + \Delta \quad (3.10)$$

The parameters $\alpha_1, \alpha_2, \alpha_3, \alpha_4$ and Δ are determined by fitting the binding energy of some nuclei, and so, their values depend somewhat on which nuclei are used for the fit. The commonly used values are [16]:

$\alpha_1 = 16 MeV$. the volume energy parameter.

$\alpha_2 = 17 MeV$. the surface energy parameter.

$\alpha_3 = 0.6 MeV$. the Coulomb energy parameter.

$\alpha_4 = 25 MeV$. the symmetry energy parameter.

Δ Is the pairing energy parameter and it is given by:

$$\Delta = \begin{cases} \delta & \text{for even - even nuclei} \\ 0 & \text{for odd mass nuclei} \\ -\delta & \text{for odd - odd nuclei} \end{cases} \quad \text{Where } \delta = \frac{25}{A} MeV$$

For infinite nuclear matter the number of nucleons (A) is infinite and the only force that acts between nucleons is the nuclear strong force as the Coulomb force is assumed to be switched off for this hypothetical system. Dividing Eq. (3.10) by A we get:

$$\frac{B(Z,N)}{A} = \alpha_1 - \frac{\alpha_2}{A^{1/3}} - \alpha_3 \frac{Z(Z-1)}{A^{4/3}} - \alpha_4 \frac{(N-Z)^2}{A^2} + \frac{\Delta}{A} \quad (3.11)$$

Eq. (3.11) gives the binding energy per particle. Note that the surface energy is proportional to $A^{-1/3}$ and since the number A is infinite for infinite nuclear matter the surface term tends to vanish.

For a hypothetical ideal system such as infinite nuclear matter all contributions from the electromagnetic effects such as Coulomb repulsion between protons are assumed to be turned off so that the Coulomb term can be put to zero. Also we assume that $N=Z$ since now the protons and neutrons have the same interaction and so the symmetry energy term can be put to zero. The Pairing effect can be ignored. Now Eq. (3.11) becomes:

$$\frac{E_B(Z,N)}{A} = \alpha_1 \quad (3.12)$$

Using the value of $\alpha_1 = 16 \text{ MeV}$, we find that the binding energy per particle of infinite nuclear matter is 16 MeV .

For finite nuclei, we use the Weizsaecker mass formula in Eq. (3.11) to show that the binding energy per particle in finite nuclei is about 8 MeV for most heavy nuclei $A > 20$. This is shown in Figure 3.1.

In plotting Figure 3.1, we derived Eq. (3.10) with respect to Z and at constant A , the value of Z that maximizes the binding energy is found as a function of A , it is given by the relation:

$$Z = \frac{4\alpha_4 A^{1/3} + \alpha_3}{2\alpha_3 + (8\alpha_4/A^{2/3})} \quad (3.13)$$

By substituting this value of Z again in Eq. (3.10) and dividing by A then this equation becomes a function of A only and it is plotted in Figure 3.1. It is seen in the figure that a sharp peak is obtained at $A=4$.

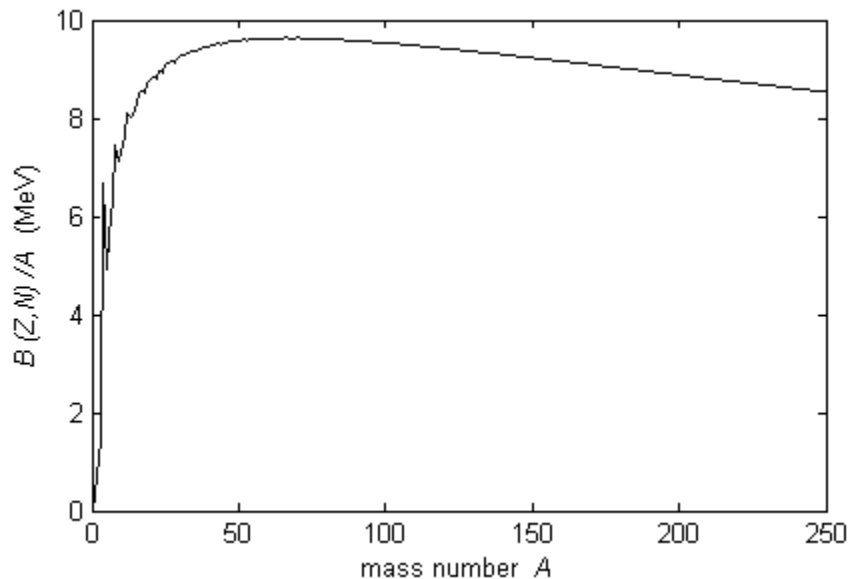


Figure 3.1: shows the binding energy per nucleon for finite nuclei, it is seen that for nuclei with mass number (A) >20 MeV the binding energy per nucleon is about 8 MeV.

Figure 3.2 next is plotted following the same procedure done in plotting Figure 3.1 but now with the pairing energy is neglected. We see also in this Figure that the binding energy per particle is about 8 MeV.

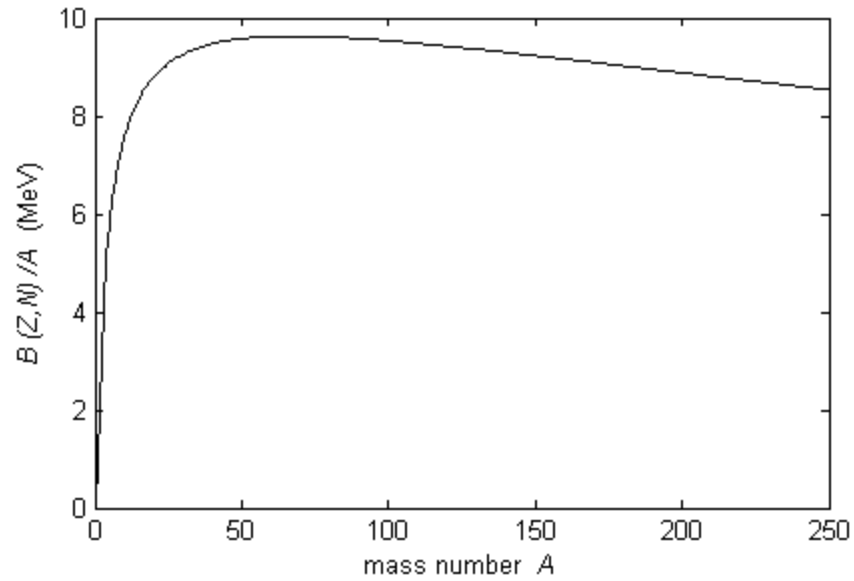


Figure 3.2: shows the binding energy per particle for finite nuclei when the pairing energy in equation (3.10) is neglected.

The experimental results of the binding energy per particle for finite nuclei are shown in Figure 3.3 [16].

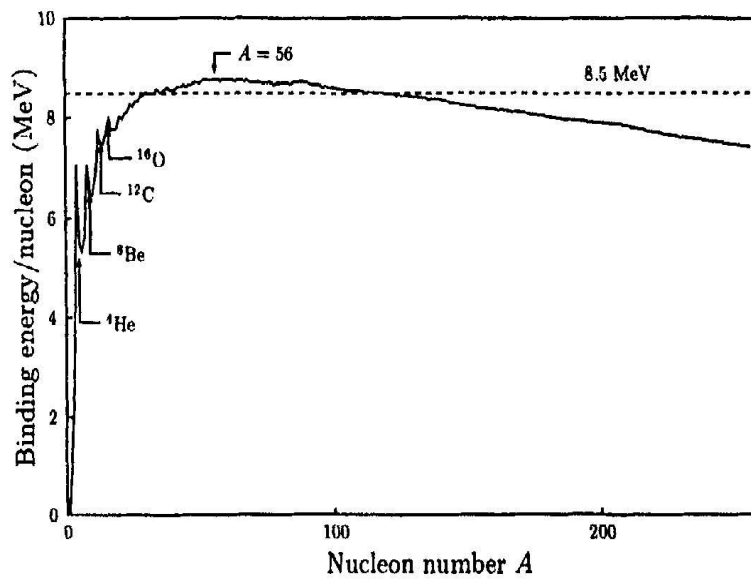


Figure 3.3: Experimental results of the binding energy per particle of finite nuclei.

The kinetic energy per particle can also be calculated. The Fermi gas model can be used to get the value of the kinetic energy per particle in infinite nuclear matter. In this model the nucleons are treated as non-interacting fermions, with the ground state formed by filling up all the available low-lying single-particle states, so that a degenerate Fermi gas is formed, and the degenerate Fermi gas model is used to describe such a system. Consider the problem of a free particle in a cubical box of length L the wavefunction is of the form

$$\Psi(\vec{r}) = \frac{1}{L^{3/2}} e^{i\vec{k}\cdot\vec{r}}$$

which is a plane wave; the \vec{k} is the wave vector of the particle and \vec{r} is the position vector. The wave vector components can be written as:

$$k_x = \frac{2\pi}{L} n_x \quad k_y = \frac{2\pi}{L} n_y \quad k_z = \frac{2\pi}{L} n_z$$

where: n_x, n_y and n_z are $0, \pm 1, \pm 2, \dots$. If the particles are nucleons, the number of allowed plane wave states in a volume element d^3k is:

$$dn = 4 \left(\frac{L}{2\pi} \right)^3 d^3k \quad \text{where the number 4 represents the spin-isospin degeneracy factor.}$$

Since we are assuming degenerate Fermi gas, the total number of nucleons A are located

$$\text{below the Fermi level, this can be written as: } A = \int_0^{\epsilon_f} dn = \int_0^{k_f} 4 \left(\frac{L}{2\pi} \right)^3 d^3k =$$

$$4 \left(\frac{L}{2\pi} \right)^3 \frac{4\pi}{3} k_f^3$$

In this relation we are assuming the ground state to form a sphere of radius k_f in momentum space where $\hbar k_f$ represents the Fermi momentum; all nucleon momenta are

located inside this sphere. Infinite nuclear matter density represents the total number of nucleons in the volume of the cubical box:

$$\rho_0 = \frac{A}{L^3} = \frac{2}{3\pi^2} k_f^3$$

From which we get:

$$k_f = \left(\frac{3\pi^2}{2} \rho_0 \right)^{1/3}$$

By substituting $\rho_0 = 0.17 \text{ fm}^{-3}$, we find the Fermi momentum $k_f = 1.36 \text{ fm}^{-1}$. Now the average kinetic energy of the nucleons can be found using the fact that the energy for a nucleon is $\varepsilon = \frac{(\hbar k)^2}{2m}$, m is the mass of the nucleon $\approx 940 \text{ MeV}$ so that:

$$\bar{\varepsilon} = \frac{1}{A} \int_0^{k_f} \frac{(\hbar k)^2}{2m} 4 \left(\frac{L}{2\pi} \right)^3 d^3 k = \frac{3}{5} \frac{(\hbar k_f)^2}{2m} = \frac{3}{5} \varepsilon_f$$

Using this relation the kinetic energy per particle of a nucleon is calculated to be 24 MeV. For comparison, the kinetic energy per particle for finite nuclei is 20 MeV [2].

3.2. EQUATION OF STATE OF A SYSTEM IN THE NUCLEONIC MODEL

In chapter (2) we have derived the equation of state of an ideal Fermi gas. This equation can be applied to a system of non-interacting nucleons at low density. It can be extended to a system in the nucleonic model in which the nucleons interact only via the Skyrme force. The only change that occurs is in the single particle energy.

The single particle energy we are using in this thesis is investigated in [14] and used in [1, 5]. It has the general form:

$$\begin{aligned} \varepsilon_q = & \frac{\hbar^2 k^2}{2m_q} - t_0 \left[\left[1 + \frac{x_0}{2} \right] \rho - \left[x_0 + \frac{1}{2} \right] \rho_q \right] \\ & + \frac{1}{4} t_3 [\rho^{1+\sigma} - \sigma \rho^{\sigma-1} \rho_q^2 + (\sigma - 1) \rho^\sigma \rho_q] + \delta_{pq} V_{Coul}(\rho) \end{aligned} \quad (3.14)$$

For symmetric nuclear matter the densities of protons and neutron are equal $\rho_p = \rho_n = \frac{\rho}{2}$, and the Coulomb term is zero. Then for symmetric nuclear matter in which protons and neutrons are treated in the same manner and called nucleons Eq. (3.14) is reduced to:

$$\varepsilon = \frac{\hbar^2 k^2}{2m} - \frac{3}{4} t_0 \rho + \frac{t_3}{8} \left(1 + \frac{\sigma}{2} \right) \rho^{1+\sigma} = \frac{\hbar^2 k^2}{2m} + \varepsilon_0 \quad (3.15)$$

where

$$\varepsilon_0 = -\frac{3}{4} t_0 \rho + \frac{t_3}{8} \left(1 + \frac{\sigma}{2} \right) \rho^{1+\sigma}$$

The chemical potential for symmetric nuclear matter with the Skyrme interaction is obtained by replacing equation (2.19) with (3.15) and repeating the same steps we followed in chapter (2). In this case we have:

$$Q(\beta) = \frac{V}{\lambda_T^3} e^{-\beta \varepsilon_0}$$

and

$$\eta = \frac{A}{gQ(\beta)} = \frac{\lambda_T^3 A}{gV} e^{\beta \varepsilon_0} = \frac{\rho}{4} \lambda_T^3 e^{\beta \varepsilon_0}$$

$$S_n(\beta) = n \frac{-3}{2} e^{-(n-1)\beta\epsilon_0}$$

Substituting these relations in the equation of state given by Eq. (2.17), the chemical potential becomes:

$$\mu = \epsilon_0 + kT \left[\ln \left(\frac{\lambda_T^3 \rho}{g} \right) + \sum_{n=1}^{\infty} b_n \left(\frac{\lambda_T^3 \rho}{g} \right)^n \right] \quad (3.16)$$

Using Eqs. (2.24) and (2.25) the pressure is found from the chemical potential; then the equation of state for symmetric nuclear matter in the nucleonic model can be rewritten as:

$$\tilde{P}(T, \rho) = -a_0 \rho^2 + a_3 (1 + \sigma) \rho^{(2+\sigma)} + T \rho \left[1 + \sum_{n=1}^{\infty} \frac{n}{n+1} b_n \left[\frac{\lambda_T^3 \rho}{g} \right]^n \right] \quad (3.17)$$

$$\tilde{\mu}(T, \rho) = -2a_0 \rho + a_3 (2 + \sigma) \rho^{(1+\sigma)} + T \left[\ln \left[\frac{\lambda_T^3 \rho}{g} \right] + \sum_{n=1}^{\infty} b_n \left[\frac{\lambda_T^3 \rho}{g} \right]^n \right] \quad (3.18)$$

where $g=4$ is the spin- isospin degeneracy factor.

Eq. (3.17) is plotted in Figure 3.4 at four different temperatures using the force with $\sigma=0.25$.

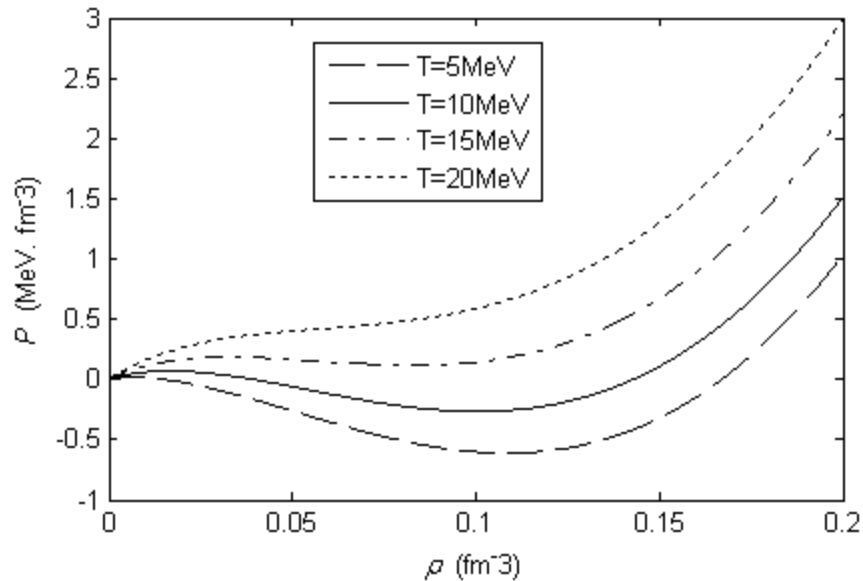


Figure 3.4: The isotherms of a system of nucleons in the nucleonic model at four different temperatures

The isotherms first rise to a maximum then drop to a minimum then rise again. The shape they form is similar to the shape of the isotherms obtained from the van der Waals equation of state. The region where the pressure has a negative slope is unphysical as the system is mechanically unstable. Each isotherm consists of three parts corresponding to the low-density vapor region, the unstable unphysical region and the high-density liquid region of the equation of state. At a certain temperature (the critical temperature) the maximum and minimum will merge and we have the critical point above which there is one fluid phase and no liquid-gas phase transition. In particular the shape of the $T=20$ MeV isotherm indicates that it is above the critical temperature.

Eq. (3.18) is plotted in Figure 3.5 for $\sigma=0.25$.

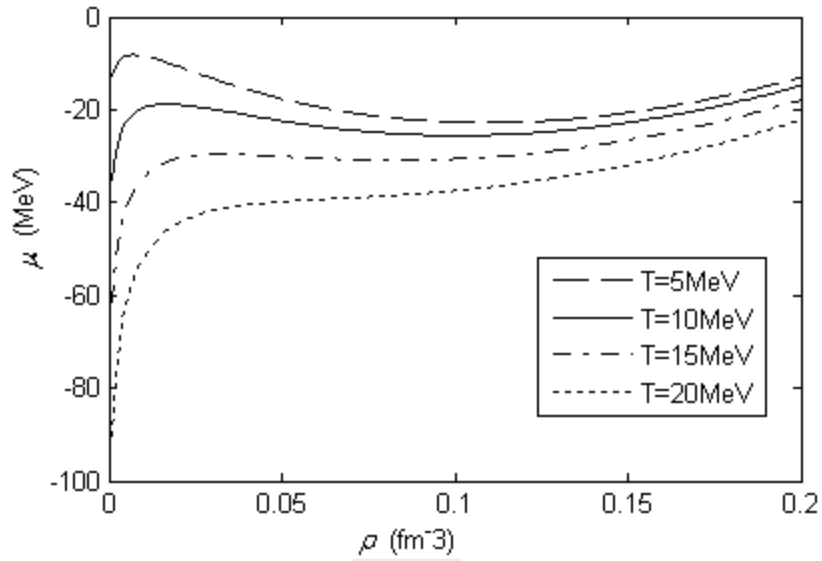


Figure 3.5: The chemical potential isotherms in the nucleonic model at four different temperatures

The chemical potential isotherms come from minus infinity rising to a maximum then they drop to a minimum, after that they rise again. At the critical temperature the maximum and minimum will merge. Above the critical temperature the chemical potential is always increasing with density.

The critical point is defined by three values (critical temperature, critical pressure, and critical density) and can be obtained from the isotherms. The critical point is the point at which the isotherm has an inflection point, and at this point we have:

$$\frac{dP}{d\rho} = \frac{d^2P}{d\rho^2} = 0 \quad \text{if we obtained it from a plot of pressure isotherms}$$

or

$$\frac{d\mu}{d\rho} = \frac{d^2\mu}{d\rho^2} = 0 \quad \text{if we obtained it from a plot of chemical potential isotherms.}$$

In the following two Figures we show how to get the critical values for the $\sigma=0.25$ force from the pressure and chemical potential isotherms:

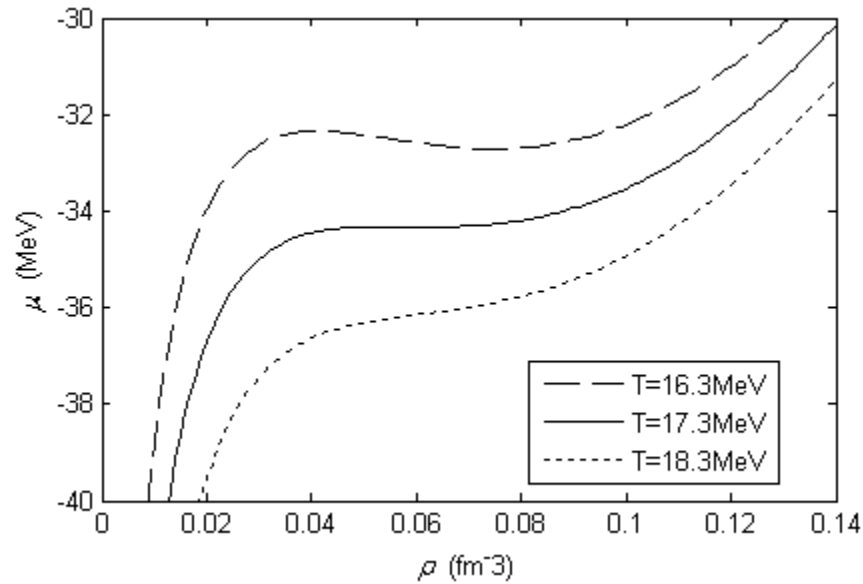


Figure 3.6: shows how to find the critical point for $\sigma = 0.25$ using a plot of chemical potential isotherms.

Figure 3.6 shows that the inflection point occurs at temperature $T=17.3$ MeV. In Figure 3.7 we are trying to find the critical temperature from the pressure isotherms.

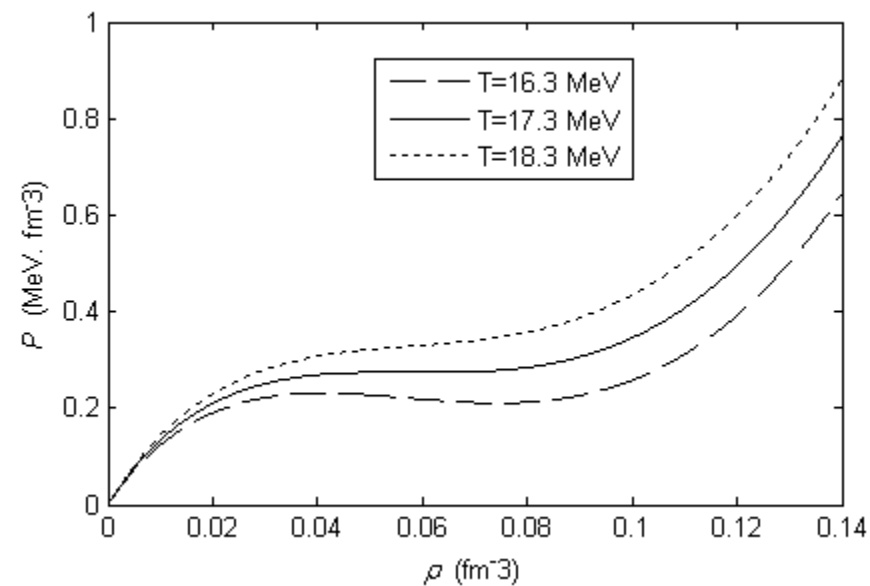


Figure 3.7: shows how to get the critical point from the pressure isotherms for $\sigma=0.25$

Figure 3.7 also shows that the critical temperature for the $\sigma=0.25$ force is 17.3 MeV. It can be seen in Figures 3.4 and 3.5 that at $T=20\text{MeV}$ which is higher than the critical temperature that the equation of state represents only one fluid phase.

In Table 3 the critical values are summarized for different values of σ . Small differences were found between our results and those obtained in [2, 5]. These differences may be attributed to the reason that in those two references the pressure series was only summed up to $n=5$, while here we are calculating the pressure series up to $n=6$.

	$\sigma=0.25$ This work	$\sigma=1$ This work	$\sigma=0.25$ [5]	$\sigma=1$ [2]
Critical temperature	17.3 MeV	22.9 MeV	17.22 MeV	22.9MeV
Critical pressure	0.2745 MeV. fm^{-3}	0.5155 MeV. fm^{-3}	0.2698 MeV. fm^{-3}	0.5151 MeV. fm^{-3}
Critical density	0.0535 Nucleon. fm^{-3}	0.064 Nucleon. fm^{-3}	0.0602 Nucleon. fm^{-3}	0.068 Nucleon. fm^{-3}

Table 3 summarizes the critical values at different σ values.

To study the effect of different parameterizations of the Skyrme interactions brought about by changing the parameter σ , Figure 3.8 below shows the pressure isotherms for $T=6$ MeV at different values of σ : $\sigma=0.25$ and $\sigma=1$. We can see that: at densities up to about $0.04 \text{ nucleon. fm}^{-3}$ the effect of changing from $\sigma=0.25$ to $\sigma=1$ is negligible. In this region the results are independent of the parametrization of the interaction. At high densities the $\sigma=1$ parameterization produces a stiffer equation of state.

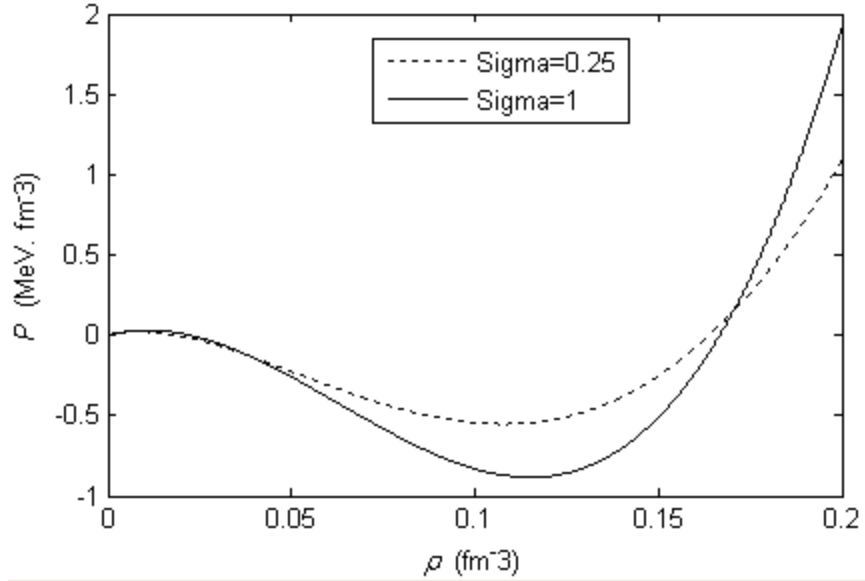


Figure 3.8: shows the effect of different Skyrme parameterizations on the equation of state.

3.3. NUCLEAR EQUATION OF STATE FOR ASYMMETRIC NUCLEAR MATTER

In asymmetric nuclear matter the protons and neutrons are treated separately and the Coulomb interaction between protons is included. To get the chemical potential for each type of nucleons the single particle energy given by Eq. (2.19) is replaced by Eq. (3.14). Also the value of A in Eq. (2.21) is replaced by Z for protons and N for neutrons. The isospin symmetry is broken for asymmetric nuclear matter because of the inclusion of the Coulomb force. The value of g now is 2 for each type and it represents the spin degeneracy factor. Finding the chemical potential for each type can be done in the same way as in obtaining Eq. (3.16). The chemical potential has the form:

$$\mu_q = \varepsilon_q + T \left[\ln \left(\frac{\lambda_T^3 \rho_q}{g} \right) + \sum_{n=1}^{\infty} b_n \left(\frac{\lambda_T^3 \rho_q}{g} \right)^n \right] \quad (3.19)$$

Where $q=p$ for protons and $q=n$ for neutrons. The single particle energy for each of the protons and neutrons is given by Eq. (3.14) which is also given in [1]:

$$\begin{aligned} \varepsilon_q = & -t_0 \left[\left[1 + \frac{x_0}{2} \right] \rho - \left[x_0 + \frac{1}{2} \right] \rho_q \right] + \frac{1}{4} t_3 [\rho^{1+\sigma} - \sigma \rho^{\sigma-1} \rho_q^2 + (\sigma - 1) \rho^\sigma \rho_q] \\ & + \delta_{pq} V_{Coul}(\rho) \end{aligned} \quad (3.20)$$

For this type of matter we define the asymmetry parameter α where:

$$\alpha = y - x$$

and

$$x = \frac{\rho_p}{\rho} = \frac{Z}{A} \quad \text{and} \quad y = \frac{\rho_n}{\rho} = \frac{N}{A}$$

Then:

$$\rho_n = \frac{\rho}{2}(1 + \alpha) \quad \text{and} \quad \rho_p = \frac{\rho}{2}(1 - \alpha)$$

A larger value of α means a larger fraction of the neutrons is in the nuclear matter.

Substituting $\rho_n = \frac{\rho}{2}(1 + \alpha)$ in Eq. (3.19) and expanding up to the second order in the asymmetry parameter α we get the neutron chemical potential:

$$\mu_n(T, \rho, \alpha) = \tilde{\mu}(T, \rho) + \mu_{n,sym}(T, \rho, \alpha) \quad (3.21)$$

where:

$$\tilde{\mu}(T, \rho) = -2a_0\rho + a_3(2 + \sigma)\rho^{(1+\sigma)} + T \left[\ln \left[\frac{\lambda_T^3 \rho}{2g} \right] + \sum_{n=1}^{\infty} b_n \left[\frac{\lambda_T^3 \rho}{2g} \right]^n \right] \quad (3.22)$$

and $\mu_{n,sym}(T, \rho, \alpha)$ is the term that comes from the asymmetry of the nuclear matter. It has the value [5]:

$$\mu_{n,sym}(T, \rho, \alpha) = \mu_1(T, \rho, \alpha) + \mu_2(T, \rho, \alpha) \quad (3.23)$$

where:

$$\mu_1(T, \rho, \alpha) = \left\{ \frac{4}{3} \left(x_0 + \frac{1}{2} \right) a_0 \rho - 2a_3 \rho^{1+\sigma} + T \left[1 + \sum_{n=1}^{\infty} n b_n \left[\frac{\lambda_T^3 \rho}{2g} \right]^n \right] \right\} \alpha \quad (3.24)$$

$$\mu_2(T, \rho, \alpha) = \left\{ -\sigma a_3 \rho^{1+\sigma} + T \left[-\frac{1}{2} + \sum_{n=1}^{\infty} \frac{(n^2 - n)}{2} b_n \left[\frac{\lambda_T^3 \rho}{2g} \right]^n \right] \right\} \alpha^2 \quad (3.25)$$

The chemical potential of the protons is obtained by substituting $\rho_p = \frac{\rho}{2}(1 - \alpha)$ in Eq. (3.19) and expanding up to the second order in the asymmetry parameter:

$$\mu_p(T, \rho, \alpha) = \tilde{\mu}(T, \rho) + \mu_{p,sym}(T, \rho, \alpha) + \mu_{Coul}(\rho) \quad (3.26)$$

where [5]:

$$\mu_{p,sym}(T, \rho, \alpha) = -\mu_1(T, \rho, \alpha) + \mu_2(T, \rho, \alpha) \quad (3.27)$$

$\mu_{Coul}(\rho)$ is the Coulomb potential energy, this term is only included if the nuclear matter is finite and this will be discussed in chapter (5) where we introduce the hot liquid drop model of the nucleus.

After determining the chemical potential of protons and neutrons it is easy now to obtain the pressure of the system using the Gibbs-Duhem relation:

$$\frac{\partial P}{\partial \rho} = x \rho \frac{\partial \mu_p}{\partial \rho} + y \rho \frac{\partial \mu_n}{\partial \rho} \quad (3.28)$$

Now the pressure of the system is given by the following equation [5]:

$$P(T, \rho, \alpha) = \tilde{P}(T, \rho) + P_{sym}(T, \rho, \alpha) + P_{Coul}(\rho) \quad (3.29)$$

where:

$$\tilde{P}(T, \rho) = -a_0\rho^2 + a_3(1 + \sigma)\rho^{(2+\sigma)} + T\rho \left[1 + \sum_{n=1}^{\infty} \frac{n}{n+1} b_n \left[\frac{\lambda_T^3 \rho}{2g} \right]^n \right] \quad (3.30)$$

is the bulk pressure of symmetric infinite nuclear matter with Skyrme interactions derived in Eq. (3.17).

$$P_{sym}(T, \rho, \alpha) = \left[\frac{2}{3} \left(x_0 + \frac{1}{2} \right) a_0 \rho^2 - (1 + \sigma) a_3 \rho^{(2+\sigma)} + T\rho \sum_{n=1}^{\infty} \frac{n^2}{2} b_n \left[\frac{\lambda_T^3 \rho}{2g} \right]^n \right] \alpha^2 \quad (3.31)$$

and $P_{Coul}(\rho)$ again is defined for finite nuclear matter.

Eq. (3.29) is the equation of state of asymmetric nuclear matter. This equation and Eqs. (3.21) and (3.26) will be used in chapter (5) to describe the nuclear matter inside and outside the hot nucleus. In chapter (6) the model will be modified to include clusters in the surrounding vapor.

CHAPTER 4. NUCLEAR STATISTICAL EQUILIBRIUM (NSE)

MODEL

Nuclear matter at densities much less than the saturation density tends to form clusters [9-13] to minimize its energy and entropy. As a result two- three- and many-body correlations are formed. This creates new bound states (clusters) which appear as new particle species in the system, change its composition and modify its thermodynamical behavior. Studies [10, 13] showed that clusters with $A= 2, 3$ and 4 are dominant at low density and so they must be included in any equation of state that describes the nuclear matter at this limit.

It was also shown in [10] that the light clusters formed in the nuclear matter get dissolved as the density of the nuclear matter increases due to the medium effects and Pauli blocking. This effect is called the Mott transition and it depends on the change of the binding energy of the clusters when placed in a medium. The density at which the cluster binding energy vanishes and the cluster dissolves is called the Mott density. Its value depends on the cluster type.

4.1. REVIEW OF THE EQUATION OF STATE OF CLUSTERED NUCLEAR MATTER IN VARIOUS MODELS

The equation of state of clustered nuclear matter has been the subject of many theoretical investigations; many approaches were used to get it:

- i. The virial expansion [9, 17] takes into account both bound states and scattering states but neglects medium modifications. In [9] this method was used to get the

equation of state of a nuclear matter composed of protons, neutrons and alpha particles at low density. It has the form:

$$\begin{aligned} \frac{P}{T} = \frac{2}{\lambda^3} [Z_n + Z_p + (Z_n^2 + Z_p^2)b_n + 2Z_pZ_nb_{pn}] \\ + \frac{1}{\lambda_\alpha^3} [Z_\alpha + Z_\alpha^2b_\alpha + 2Z_\alpha(Z_n + Z_p)b_{\alpha n}] \end{aligned} \quad (4.1)$$

where: λ_α^3 and λ^3 are the thermal wave lengths of alpha particles and nucleons respectively, $Z_n = e^{\frac{\mu_n}{T}}$ and $Z_p = e^{\frac{\mu_p}{T}}$ are the fugacities of neutrons and protons respectively and $Z_\alpha = e^{\frac{\mu_\alpha + E_\alpha}{T}}$ is the fugacity of alpha, E_α is the binding energy of alpha particles.

The coefficient b_n is the second nucleon virial coefficient and b_α is the second alpha virial coefficient. The coefficients $b_{\alpha n}$ and b_{pn} are the virial coefficients that describe the strong interactions between the particles. All the four virial coefficients are calculated in [9] using nn, pp, np, n α , p α and $\alpha\alpha$ elastic scattering phase shifts.

- ii. The Microscopic quantum statistical approach used in [10, 11].

The Microscopic calculations arise from a model that describes the interactions between nucleons in a system, such interaction is the formation of the bound states at low density nuclear matter. The quantum statistical approach is a non-relativistic approach that is based on the many body theory. It makes an explicit use of the effective nucleon-nucleon interactions and takes into account the medium effects of the cluster properties such as the Mott density at which the clusters dissolve.

In this approach the nucleons and clusters are treated as quasi-particles, the quasi-particle energy of a cluster with Z protons and N neutrons in the ground state is given in [10, 11]:

$$E_{A,Z}^{qu}(P) = E_{A,Z}^{(0)} + \frac{P^2}{2Am} + \Delta E_{A,Z}^{SE}(P) + \Delta E_{A,Z}^{Pauli}(P) + \Delta E_{A,Z}^{Coul}(P) + \dots \quad (4.2)$$

where m is the mass of the nucleon, and P is the momentum of the cluster. The five terms of Eq. (4.2) are explained as follows:

$E_{A,Z}^{(0)}$ is the cluster binding energy in vacuum.

$\frac{P^2}{2Am}$ is the kinetic energy of the cluster.

$\Delta E_{A,Z}^{SE}(P)$ is the shift that occurs in the self energy due to the medium effects where the self energy is the potential felt by the cluster. This potential represents all interactions between the cluster and all other clusters and nucleons in the system. The value of this shift is evaluated from the change in the effective mass of the cluster quasi-particle.

$\Delta E_{A,Z}^{Coul}(P)$ is the Coulomb term, this term is small and negligible for symmetric nuclear matter.

$\Delta E_{A,Z}^{Pauli}(P)$ is the Pauli blocking term. It is given in [10] at zero center of mass momentum:

$$\Delta E_{A_i, Z_i}^{Pauli}(0; n_p, n_n, T) = \frac{-2}{A_i} [Z_i n_p + N_i n_n] \delta E_i^{Pauli}(T, n) \quad (4.3)$$

where:

$$\delta E_i^{Pauli}(T, n) = \frac{a_{i,1}}{T^{3/2}} \frac{1}{y_i^{3/2}} \frac{1}{1 + [b_{i,1} + b_{i,2}/T]n} \quad \text{when applied on tritons, helions, and}$$

alphas, and it has the value:

$$\delta E_i^{Pauli}(T, n) = \frac{a_{i,1}}{T^{3/2}} \left[\frac{1}{\sqrt{y_i}} - \sqrt{\pi} a_{i,3} \exp(a_{i,3}^2 \sqrt{y_i}) \operatorname{erfc}(a_{i,3} \sqrt{y_i}) \right] \times \frac{1}{1 + [b_{i,1} + b_{i,2}/T]n}$$

when applied on deuterons.

where: $y_i = 1 + \frac{a_{i,2}}{T}$, the parameters $a_{i,1}$, $a_{i,2}$ and $a_{i,3}$ are determined by the low density perturbation theory, and the parameters $b_{i,1}$ and $b_{i,2}$ represent the density corrections. We can see that the Pauli blocking is inversely proportional to the $T^{3/2}$. As a result, this term becomes smaller at higher temperatures.

A great attention is devoted in [10, 11] to the Pauli blocking term because it is the main medium effect that enters in the calculations of the abundance of light clusters at low density nuclear matter. Pauli blocking is restricted only to bound states, it acts on the clusters, decreases their binding energies as the density of the medium increases. At the Mott density the binding energy of the cluster goes to zero and the cluster becomes unbound. For every type of cluster there is a characteristic Mott density which is affected by the center of mass momentum of the cluster and depends on the temperature. The most weakly bound cluster dissolves first.

- iii. The NSE model used in [13, 18, 19] which takes into account only bound states and it is the model we are using in this thesis with some modifications involving a density-dependent binding energy.

4.2. THE NUCLEAR STATISTICAL EQUILIBRIUM (NSE) MODEL

The NSE [13, 18, 19] treats the nuclear matter from a statistical view; it describes the nuclear matter at low density as a system of non-interacting or minimally interacting particles at statistical equilibrium. This model takes into account only the bound states; it

ignores other scattering and excited states. It gives the correct low density limit to which all other equations of state must terminate [10, 13, 18, 19].

In this work we will derive the equation of state for an infinite uniform distribution of symmetric clustered nuclear matter at low density. This matter is composed of fermions (nucleons, tritons and helions) and bosons (deuterons and alpha particles). These components are treated using Fermi or Bose statistics as applicable. Such a system is best described in the NSE. The original NSE takes into account only the bound states neglecting all other effects of scattering states and medium effects which are attributed mainly to the Pauli Blocking of states that changes the binding energy and causes the dissolution of clusters at the Mott density. As the density increases toward the Mott density, the binding energy decreases until it reaches zero and then the clusters dissolve.

The NSE model in its original form predicts that [10] most nucleons in symmetric nuclear matter at high density would be bound into clusters, this case is unphysical because medium modifications are not included in this model. To substitute for this deficiency in the model we will assume the binding energy to have an exponential dependence on the total density, the binding energy will be of the form:

$$B = B_0 \exp(-\rho/\rho_M(0)) \quad (4.4)$$

where:

B_0 is the binding energy of the cluster at zero density and $\rho_M(0)$ is the Mott density at zero center of mass momentum.

The binding energies at zero density for the clusters that are used in this work are found in [20] and summarized in Table 4.

	Alpha	Deuteron	Helion	Triton
B_0 (MeV)	28.295660	2.224560	7.718043	8.481798
g	1	3	2	2
Mass MeV/c^2	3728.40	1876.12	2809.41	2809.43

Table 4 summarizes the binding energy, masses and the spin degeneracy factors of some light clusters.

In [10] the shift in the binding energy due to medium modifications is studied. A linear fit of the results obtained in this reference enables us to get the $\rho_M(0)$ for different clusters, at different temperatures. The results are summarized in Table 5 at typical temperatures.

	T=2MeV	T=4MeV	T=5MeV	T=6MeV
Alpha	0.0059 fm ⁻³	0.0073 fm ⁻³	0.0080 fm ⁻³	0.0088 fm ⁻³
Deuteron	0.00148 fm ⁻³	0.00216 fm ⁻³	0.0025 fm ⁻³	0.0029 fm ⁻³
Helion	0.0023 fm ⁻³	0.0031 fm ⁻³	0.0035 fm ⁻³	0.0040 fm ⁻³
Triton	0.0028 fm ⁻³	0.0036 fm ⁻³	0.0036 fm ⁻³	0.0046 fm ⁻³

Table 5 shows the Mott densities $\rho_M(0)$ for various clusters at typical temperatures.

In Table 5 the dependence of ρ_M on the temperature is obvious, it increases with increasing temperature, this means that at high temperatures the clusters will live even at high densities. This result is expected because Pauli blocking is less effective at higher temperatures as concluded from Eq. (4.3).

Clusters in nuclear matter are at chemical equilibrium with nucleons such that:

$$\mu_{cluster} = Z\mu_p + N\mu_n \quad (4.5)$$

Because of the symmetry of the nuclear matter assumed, the chemical potentials of protons and neutrons are equal $\mu_p = \mu_n = \mu$ so that:

$$\mu_{cluster} = A\mu.$$

where: $A=N+Z$.

As a result the chemical potentials of the light clusters are written as:

$$\mu_{alpha} = 4\mu$$

$$\mu_{deuteron} = 2\mu$$

$$\mu_{helion} = 3\mu$$

$$\mu_{triton} = 3\mu$$

The chemical potential μ of free nucleons is calculated using the equation of state derived earlier in chapter (2) for an infinite system of non-interacting nucleons at low density:

$$\mu(T, \rho_{free}) = k_b T \left(\ln \left(\frac{\lambda_T^3 \rho_{free}}{g} \right) + \sum_{n=1}^{\infty} b_n \left(\frac{\lambda_T^3 \rho_{free}}{g} \right)^n \right)$$

where $k_b T$ gives the temperature in energy units, and ρ_{free} represents the density of free nucleons.

The total density of such clustered nuclear matter contains all contributions from nucleons and clusters; it is given by:

$$\rho_{total} = \rho_{free} + 4\rho_{alpha} + 3\rho_{triton} + 3\rho_{helion} + 2\rho_{deuteron} \quad (4.6)$$

The density of each type of cluster is calculated using the relation:

$$\rho_C = \frac{N}{V} = \frac{g}{(2\pi)^3} \int d^3q n_C \quad (4.7)$$

where g is the spin degeneracy factor of the cluster. The values that g takes for each type of cluster of interest are summarized in Table 4. Also in Eq. (4.7) n_C is the probability of finding cluster C with the kinetic energy ε_C^0 .

$$n_C = \{exp[\beta(\varepsilon_C^0 - \mu_C - B_C)] \pm 1\}^{-1} \quad (4.8)$$

where the (+) sign is used for fermionic clusters (helions and tritons) while the (-) sign is used for bosons (alphas and deuterons). B_C is the density-dependent binding energy of the cluster when embedded in the vapor as given by Eq. (4.4).

As shown in Eq. (4.4) the binding energy is a function of the total density which is the final result of the calculation. In order to calculate the binding energy many iterative operations are performed to achieve self consistency. The value of the total density that achieves self consistency is then used to get the binding energy of the clusters and to find the density of each type of clusters in the nuclear matter. The masses of some light clusters in energy units are summarized in table 4 they are the same values used in [12].

Now the composition of nuclear matter at low density can be determined. After calculating the density of each type of clusters and the total density which forms the final output, the fraction of nucleons existing in each type of clusters can be evaluated:

$$X_{alpha} = 4 \frac{\rho_{alpha}}{\rho_{total}}$$

$$X_{Deuteron} = 2 \frac{\rho_{Deuteron}}{\rho_{total}} \quad (4.9)$$

$$X_{helion} = 3 \frac{\rho_{helion}}{\rho_{total}}$$

$$X_{triton} = 2 \frac{\rho_{triton}}{\rho_{total}}$$

Figures 4.1 and 4.2 show the fractions of nucleons existing in clusters versus total density at two different temperatures.

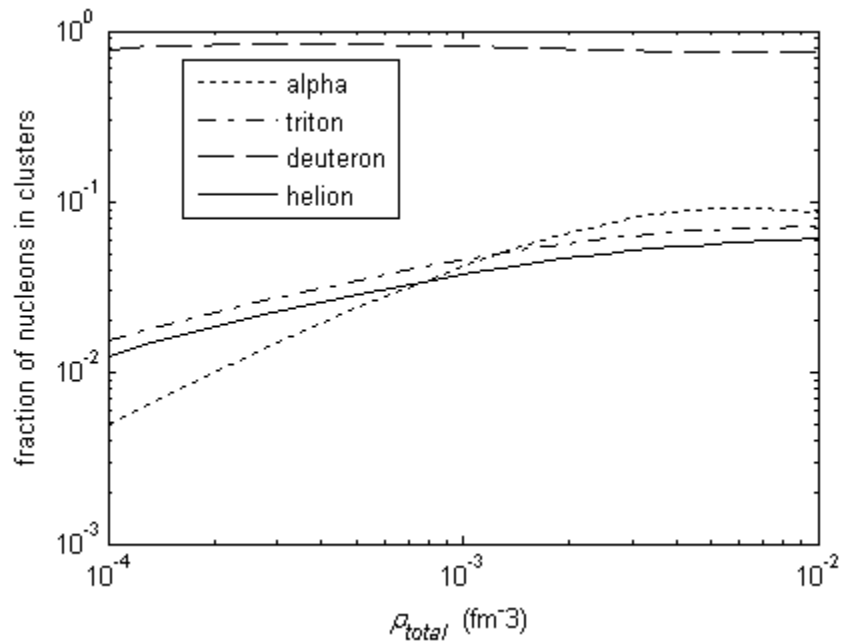


Figure 4.1: shows the abundances of nucleons existing in clusters at T=4MeV using the (NSE) model.

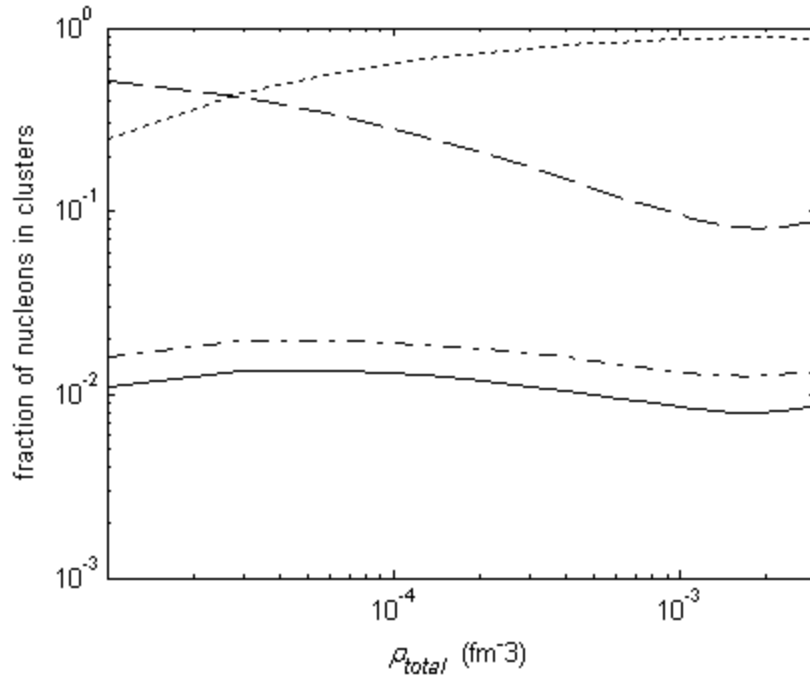


Figure 4.2: shows the abundances of nucleons existing in clusters at $T=2\text{MeV}$ in the (NSE) model.

The deuterons are dominant at $T=4\text{MeV}$ while the alpha particles are dominant at $T=2\text{MeV}$ and lower. Also, in Figure 4.2 the abundance of the lighter clusters decreases as the density increases. This occurs as a result of the change in the binding energy assumed in Eq. (4.4). The most tightly bound alpha particles live to higher values of density. We can say that at low temperatures and low densities the nuclear matter is composed mainly of deuterons and alpha particles.

4.3. EQUATION OF STATE OF CLUSTERED NUCLEAR MATTER IN THE NSE MODEL

The pressure of clustered nuclear matter contains contributions from all its contents. After calculating the density of each type of clusters the partial pressure is calculated for each type of clusters and nucleons using the ideal Fermi and Bose equations of state

derived in chapter (2). The total pressure of clustered nuclear matter in the NSE model has the form:

$$P = P_{free} + P_{clusters} \quad (4.10)$$

Figure 4.3 shows the isotherms of clustered nuclear matter at low density in the NSE model at two different temperatures. It shows that the pressure increases as the temperature increases. For comparison we also show in Figure 4.3 the isotherms obtained assuming that low density nuclear matter consists only of nucleons interacting via the Skyrme force (the nucleonic vapor model). These isotherms are plotted using the equation of state Eq. (3.17).

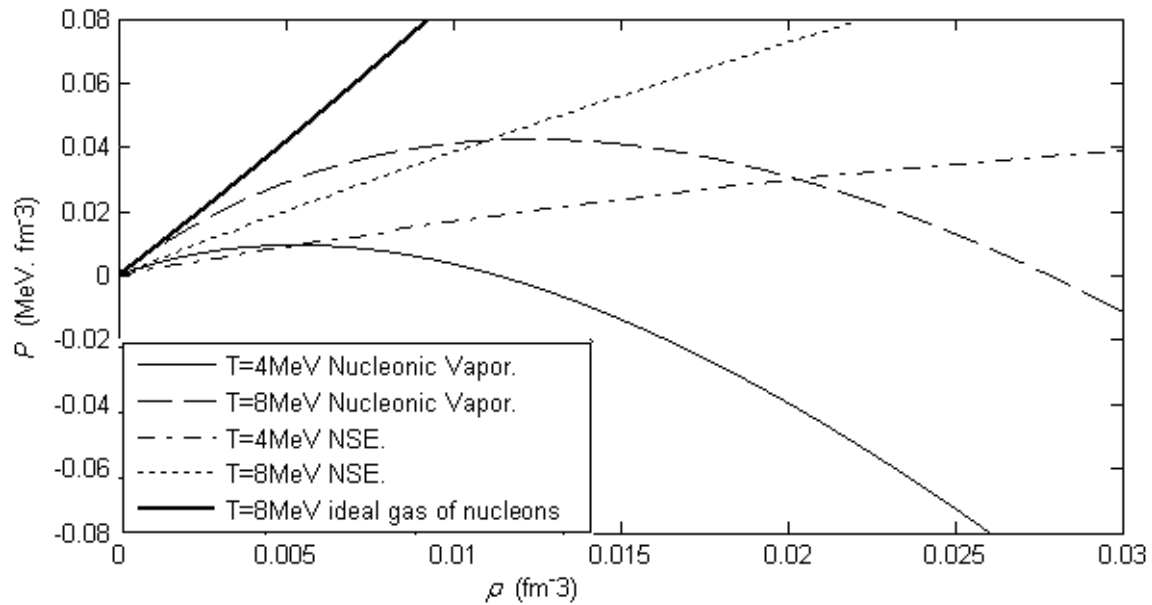


Figure 4.3: the equation of state of nuclear matter in three different models.

We see that at a certain temperature $T=8$ MeV for example, and densities much less than the saturation density 0.17 fm^{-3} the vapor pressure when clusters are included (NSE) is much less than when only nucleons are included (nucleonic vapor). Also

plotted in Figure 4.3 is the pressure of the ideal gas of nucleons at $T=8\text{MeV}$. We also note that the pressure of the system consisting of only nucleons approaches the ideal gas limit at extremely low-densities, but that the pressure of clustered nuclear matter does not because of the presence of the clusters and the implied interactions between them and the nucleons.

CHAPTER 5. LIQUID DROP MODEL FOR A HOT NUCLEUS AND THE LIMITING TEMPERATURE

Nuclear models are different ways of looking at the nucleus to describe its physical behavior and give physical explanation of a wide range of its properties. The two nuclear models that are widely used and that have proved useful are the independent particle model and the liquid drop model [16].

In the independent particle model each nucleon moves independently of the other nucleons. Each nucleon has its own wavefunction, has a definite set of quantum numbers, obeys the Pauli Exclusion Principle, and hardly makes any collision with other nucleons.

This is not the case in the liquid drop model where nucleons are assumed to move randomly inside the nucleus and make frequent collisions with each others. The Weizsaecker mass formula that was used in chapter (3) to find the binding energy of a nucleus is a consequence of the liquid drop model at zero temperature.

5.1. THE HOT LIQUID DROP MODEL

In the liquid drop model the nucleus is described as a drop of liquid with uniform density, a sharp edge, and a surface tension. The volume of this drop is proportional to A (the number of nucleons in the nucleus). The forces acting on the nucleons located in the interior of the nucleus differ from those that acting on the nucleons that are near the surface. This produces the surface tension which tends to pull the surface nucleons to the interior of the nucleus and minimizes its surface area.

In this thesis we are assuming that the hot nucleus is a uniformly charged drop with uniform density, a sharp edge, and a surface tension surrounded by a vapor. The liquid drop is in thermal, mechanical, and chemical equilibrium with the surrounding vapor. The bulk matter inside the nucleus is asymmetric with the coulomb repulsion acting between the protons. The equation of state derived earlier in chapter (3) for asymmetric nuclear matter is used here to describe the bulk matter inside the nucleus.

In asymmetric nuclear matter the protons and neutrons are treated differently. The inclusion of the Coulomb force in this matter breaks the isospin symmetry so that the factor g in this case is called the spin degeneracy factor and has a value of 2. For this matter Eqs. (3.21), (3.26) and (3.29) derived earlier in chapter (3) will be used:

The chemical potential of neutrons is given by:

$$\mu_n(T, \rho, \alpha) = \tilde{\mu}(T, \rho) + \mu_{n,sym}(T, \rho, \alpha) \quad (5.1)$$

And the chemical potential of protons is given by:

$$\mu_p(T, \rho, \alpha) = \tilde{\mu}(T, \rho) + \mu_{p,sym}(T, \rho, \alpha) + \mu_{Coul}(\rho) \quad (5.2)$$

Where: $\tilde{\mu}(T, \rho)$, $\mu_{n,sym}(T, \rho, \alpha)$ and $\mu_{p,sym}(T, \rho, \alpha)$ all were defined in chapter (3) in Eqs. (3.22), (3.23) and (3.26) respectively.

$\mu_{Coul}(\rho)$ is the Coulomb potential energy, for a uniformly charged spherical drop of radius R this potential is given by:

$$\mu_{Coul}(\rho) = V_{Coul}(\rho) = \frac{6}{5} Z e^2 \frac{1}{R} = \frac{6}{5} Z e^2 \left[\frac{4\pi\rho}{3A} \right]^{1/3} \quad (5.3)$$

The pressure of the system is given by:

$$P(T, \rho, \alpha) = \tilde{P}(T, \rho) + P_{sym}(T, \rho, \alpha) + P_{Coul}(\rho)$$

Where : $\tilde{P}(T, \rho)$ and $P_{sym}(T, \rho, \alpha)$ are given by Eqs. (3.30) and (3.31) respectively. The $P_{Coul}(\rho)$ term results from the coulomb interaction, for a uniformly charged spherical drop of radius R this pressure is given by:

$$P_{Coul}(\rho) = \left[\frac{4\pi\rho}{3A} \right]^{1/3} \frac{Z^2 e^2}{5A} \rho \quad (5.4)$$

For the pressure inside the liquid drop there is still another contribution that is due to the surface tension of the nucleus. The expression that is used to describe the surface tension must depend on the temperature and must vanish at the critical temperature which is determined by the equation of state. The critical temperature gives the main relationship between the surface tension and the equation of state which is affected by the effective interaction. The most widely used expression for the surface tension which is suggested in [21] and is used in [5] is given by:

$$\gamma(T) = 1.14 \text{ MeV} \cdot \text{fm}^{-2} \left(1 + \frac{3}{2} \frac{T}{T_c} \right) \left(1 - \frac{T}{T_c} \right)^{3/2} \quad (5.5)$$

The surface tension represents the work required to increase the surface area of the liquid drop by a certain amount. It has the unit of (energy unit) / (area unit).

The number $1.14 \text{ MeV} \cdot \text{fm}^{-2}$ gives the surface tension at zero temperature. This number is obtained from the semi-empirical mass formula (Weizsaecker mass formula) which is given in chapter (3). This formula gives the binding energy of nuclei at zero temperature.

Other studies [3] used another expression for the surface tension:

$$\gamma(T) = 1.14 \text{MeV} \cdot \text{fm}^{-2} \left(1 - \frac{T}{T_c}\right)^2 \quad (5.6)$$

Both representations of the surface tension are temperature dependent and they vanish as $T \rightarrow T_c$. However Eq. (5.5) has the correct quadratic dependence on T at low temperatures. It gives a lower value of the surface tension at low temperatures than that given by Eq. (5.6) which has a linear dependence on T . It was also shown in [7] that the limiting temperature depends on the temperature dependence of the surface tension, and that the limiting temperature calculated with Eq. (5.5) has better agreement with the results of Hartree-Fock calculations. In this work we are using Eq. (5.5) also to simplify comparison between our results and that of [5].

The pressure inside the liquid drop that is related to the surface tension is given by:

$$P_{surf}(T, \rho) = -2\gamma(T) \frac{1}{R} = -2\gamma(T) \left[\frac{4\pi\rho}{3A}\right]^{1/3} \quad (5.7)$$

Now the pressure inside the liquid drop is given by:

$$P(T, \rho, \alpha) = \tilde{P}(T, \rho) + P_{sym}(T, \rho, \alpha) + P_{Coul}(\rho) + P_{surf}(T, \rho) \quad (5.8)$$

In Figure 5.1 $\tilde{P}(T, \rho)$ as given by Eq. (3.30) and Eq. (5.8) is plotted with and without the symmetry terms. In this plot we must differentiate between two types of pressure isotherms: the bulk pressure $\tilde{P}(T, \rho)$ which is given by Eq. (3.30) and the pressure inside the drop which is obtained from the corresponding bulk pressure by adding the Coulomb and surface terms, and is given by Eq. (5.8). For the surrounding vapor phase Eq. (5.8) can be used as in [5] but without the surface term and without the

Coulomb term. The Coulomb term diverges if the vapor is assumed to be infinite. This can be remedied by assuming the vapor to be contained within a certain radius [7].

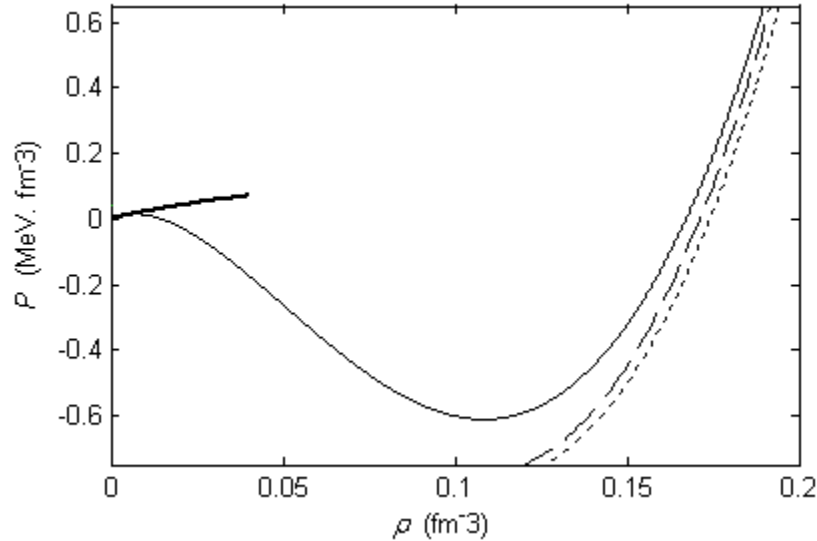


Figure 5.1: The vapor, bulk and drop isotherms at $T=5\text{MeV}$ and $\sigma=0.25$ for $^{109}_{47}\text{Ag}$ nucleus. The thin continuous line represents the bulk isotherm. The dashed line represents the drop isotherm without symmetry terms. The dotted line represents the drop isotherms with symmetry terms. The thick continuous line represents the vapor phase with clusters.

The bulk curve in Figure 5.1 consists of three parts corresponding to the vapor phase at low densities, the liquid phase which starts at densities slightly above 0.1fm^{-3} and the unstable region with negative $(\partial P/\partial\rho)$ (and hence negative compressibility) of the equation of state. The first part extends to a density about 0.015fm^{-3} and represents the vapor phase in the nucleonic vapor model. This model describes the case where the interactions assumed are of the Skyrme type and the clusters are not included. The thick solid line represents the vapor pressure in the NSE model where the clusters are included and the only interaction between nucleons is by forming clusters. The case with clusters will be treated in chapter 6.

Figure 5.2 shows the same plots of Figure 5.1 but for the nucleus $^{208}_{82}\text{Pb}$.

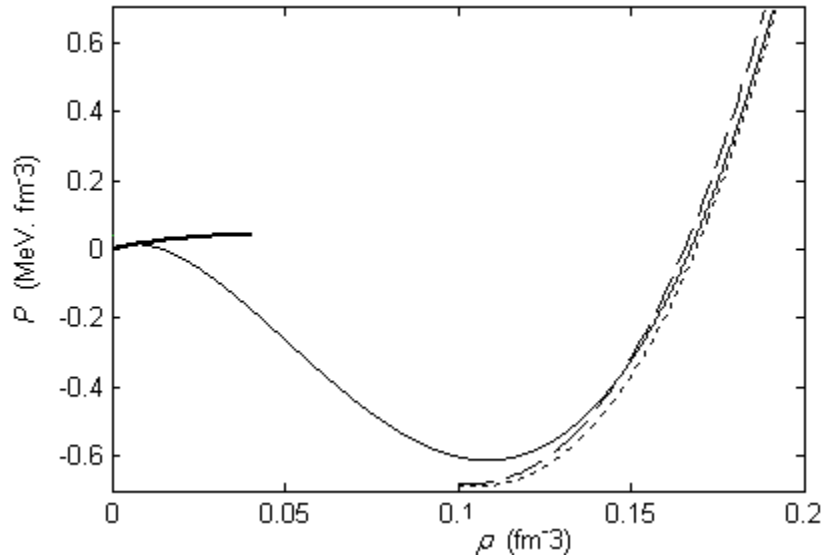


Figure 5.2: The vapor, bulk and drop isotherms for the nucleus $^{208}_{82}\text{Pb}$ at $T=5\text{MeV}$. The labels of the curves are the same as in Figure 5.1.

5.2. THE COEXISTENCE EQUATIONS

In this thesis we are dealing with the problem of the Coulomb instability of hot nuclei embedded in a vapor of nuclear matter. The nuclei that are immersed in the vapor are treated as hot liquid drops. They are assumed to exist in thermal, mechanical, and chemical equilibrium with the surrounding vapor. The mechanical equilibrium requires the equality of the pressure inside and outside the hot nucleus, and the chemical equilibrium requires the equality of the individual chemical potential of protons and neutrons inside and outside the hot nucleus. These equilibrium conditions are described in the following coexistence equations:

$$P(T, \rho_l, \alpha_l) = P(T, \rho_v, \alpha_v) \quad (5.9.a)$$

$$\mu_n(T, \rho_l, \alpha_l) = \mu_n(T, \rho_v, \alpha_v) \quad (5.9.b)$$

$$\mu_p(T, \rho_l, \alpha_l) = \mu_p(T, \rho_v, \alpha_v) \quad (5.9.c)$$

Where: ρ_l and ρ_v are the densities and α_l and α_v are the asymmetry parameters of the liquid and vapor respectively. The coulomb term is included when describing the pressure and chemical potential of protons inside the liquid drop and is neglected when describing the protons in the vapor.

In [5] the author discussed the Coulomb instability of hot nuclei embedded in a vapor. The liquid drop model was used to describe the hot nuclei. The vapor at which the hot nuclei are immersed was assumed to be uncharged asymmetric nuclear matter composed only of protons and neutrons where the interaction assumed between nucleons is of the Skyrme type. The coexistence Eqs. (5.9) for this case are written as:

$$\tilde{P}(T, \rho_l) + P_{sym}(T, \rho_l, \alpha_l) + P_{Coul}(\rho_l) + P_{surf}(T, \rho_l) \quad (5.10.a)$$

$$= \tilde{P}(T, \rho_v) + P_{sym}(T, \rho_v, \alpha_v)$$

$$\tilde{\mu}(T, \rho_l) + \mu_{n,sym}(T, \rho_l, \alpha_l) = \tilde{\mu}(T, \rho_v) + \mu_{n,sym}(T, \rho_v, \alpha_v) \quad (5.10.b)$$

$$\tilde{\mu}(T, \rho_l) + \mu_{p,sym}(T, \rho_l, \alpha_l) + \mu_{Coul}(\rho_l) = \tilde{\mu}(T, \rho_v) + \mu_{p,sym}(T, \rho_v, \alpha_v) \quad (5.10.c)$$

We see that the coexistence equations in (5.10) contain the symmetry terms that are added to both the drop and vapor equations. In the coming discussion we will show that the symmetry corrections added to the vapor equations have a negligible effect on the value of the limiting temperature. This is expected because of the small values that the vapor asymmetry parameter has. This means that we can neglect these symmetry corrections and include only the symmetry terms added to the drop equations. This result does not contradict with that reported previously in [5] where the asymmetry parameter

had values near 1. These large values of the asymmetry parameter are attributed to some numerical errors that are corrected here in the following discussion.

Returning to the set of equations (5.10) we write $\mu_{n,sym}$ and $\mu_{p,sym}$ in terms of μ_1 and μ_2 as given in Eqs. (3.23) and (3.27)., adding and subtracting the second and third equations then we can write these coexistence equations in the form:

$$\tilde{P}(T, \rho_l) + P_{sym}(T, \rho_l, \alpha_l) + P_{Coul}(\rho_l) + P_{surf}(T, \rho_l) \quad (5.11.a)$$

$$= \tilde{P}(T, \rho_v) + P_{sym}(T, \rho_v, \alpha_v)$$

$$\tilde{\mu}(T, \rho_l) + \mu_2(T, \rho_l, \alpha_l) + \frac{1}{2} \mu_{Coul}(\rho_l) = \tilde{\mu}(T, \rho_v) + \mu_2(T, \rho_v, \alpha_v) \quad (5.11.b)$$

$$\mu_1(T, \rho_l, \alpha_l) - \frac{1}{2} \mu_{Coul}(\rho_l) = \mu_1(T, \rho_v, \alpha_v) \quad (5.11.c)$$

5.3. THE LIMITING TEMPERATURE

To find the limiting temperature, the above coexistence equations Eqs. (5.11) must be solved; the limiting temperature is characterized as the temperature above which the coexistence equations have no real solution.

We will follow the procedure that is suggested in [3] and is used in [5] to obtain the limiting temperature and we can summarize it in three steps:

- I. The chemical potential of the vapor (RHS of Eq. (5.11.b)) is plotted against the corresponding pressure of the vapor (RHS of Eq. (5.11.a)).
- II. On the same graph, the chemical potential of the drop (LHS of Eq. (5.11.b)) is plotted against the corresponding pressure of the drop (LHS of Eq. (5.11.a)).

III. The coexistence equations have real solution if the drop and vapor curves intersect. This occurs below the limiting temperature and means that we have liquid - gas coexistence; above the limiting temperature the drop curve and the vapor curve do not intersect.

The calculations to find the limiting temperature will be divided into two parts:

- 1- Solving the coexistence equations (5.11) with the asymmetry corrections added to the drop equations are taken into account while those added to the vapor equation are neglected.
- 2- Solving the coexistence equations (5.11) exactly.

In the first part of the calculations we will take into account the asymmetry terms added only to the drop equations. This means neglecting the asymmetry corrections on the right hand side of the Eqs. (5.11.a) and (5.11.b) which thus become decoupled from Eq. (5.11.c). Next, Eqs. (5.11.a) and (5.11.b) are solved without the vapor asymmetry corrections and the vapor asymmetry parameter is calculated using Eq. (5.11.c).

Figure 5.3 below shows the relationship at $T=5\text{MeV}$ and $\sigma=0.25$ between the chemical potential and the pressure in the bulk for the case of a drop representing a ${}^{109}_{47}\text{Ag}$ nucleus. In this Figure the asymmetry terms are only added to the drop equations.

The bulk isotherm consists of three regions shown in the Figure; the vapor region, the unstable region, and the liquid (bulk) region. The drop and vapor isotherms intersect at the equilibrium point which means that at this point we have liquid -gas coexistence and the nucleus or liquid drop exists in equilibrium with its surrounding vapor. It is easy to see that $T=5\text{MeV}$ is below the limiting temperature.

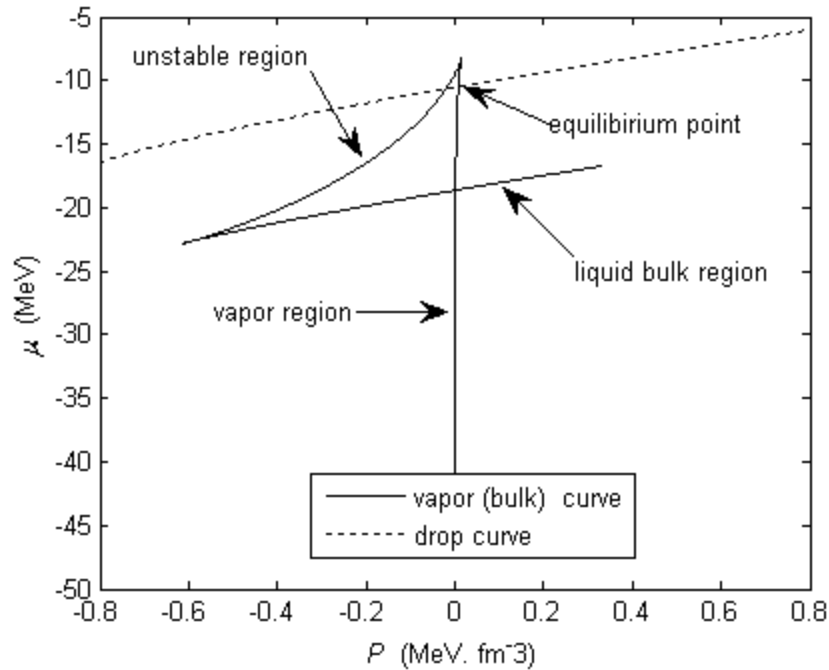


Figure 5.3: The bulk and drop pressure versus chemical potential at $T=5\text{MeV}$ and $\sigma=0.25$ for $^{109}_{47}\text{Ag}$ with the asymmetry terms added to the drop equations only.

Figure 5.4 shows that the limiting temperature for the $^{109}_{47}\text{Ag}$ case is $T=6.8\text{MeV}$.

5.4. EVALUATING THE VAPOR ASYMMETRY PARAMETER.

For a given temperature (here $T=6.8\text{ MeV}$) the vapor asymmetry parameter is calculated as follows:

First: The chemical potential and pressure at the equilibrium point are determined from Figure 5.4. They have the values: -12.05 MeV for the chemical potential and $0.02978\text{ MeV}\cdot\text{fm}^{-3}$ for the pressure.

Second: The values of the vapor and liquid densities at the equilibrium point are determined. They have the values $\rho_l = 0.1682\text{ fm}^{-3}$ and $\rho_v = 0.0100\text{ fm}^{-3}$.

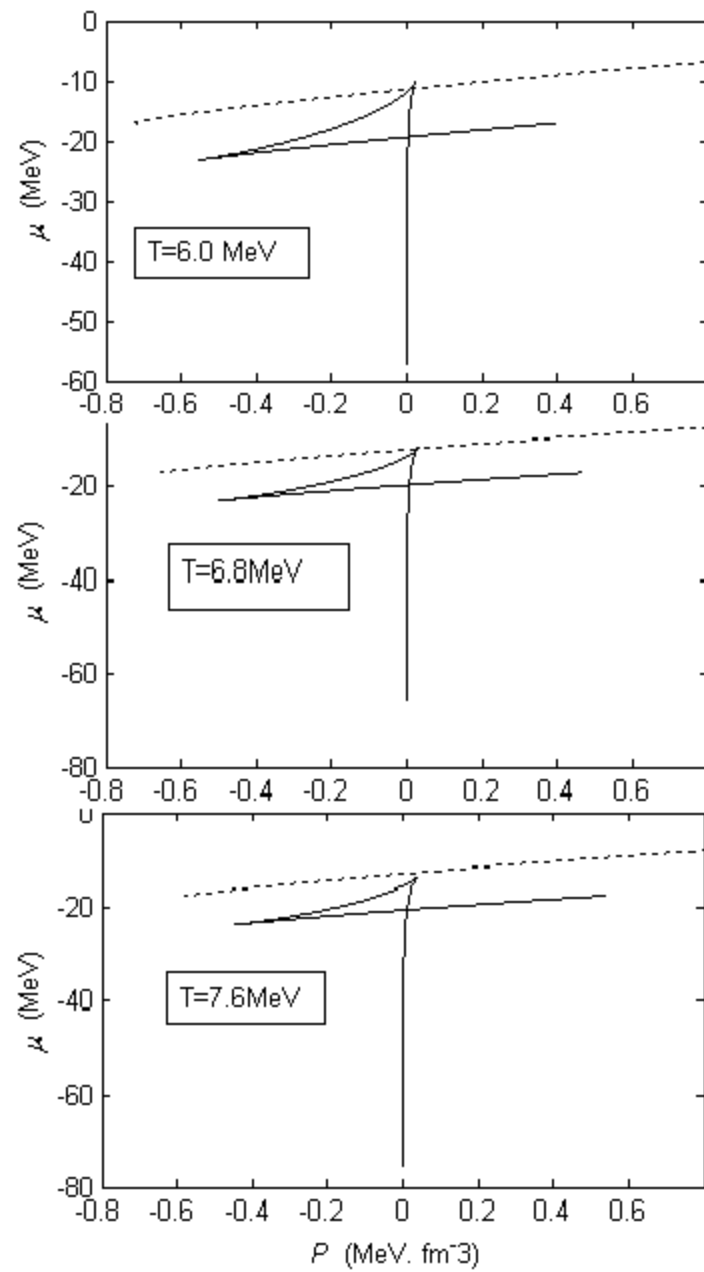


Figure 5.4 shows that the limiting temperature for the $^{109}_{47}\text{Ag}$ nucleus when $\sigma=0.25$ is $T=6.8$ MeV.

Third: a plot the left hand side of Eq. (5.11.c) as a function of the density of liquid ρ_l is shown in Figure 5.5. It is seen that the left hand side of Eq. (5.11.c) does not vary in going from density (0.165 - 0.175) fm^{-3} .

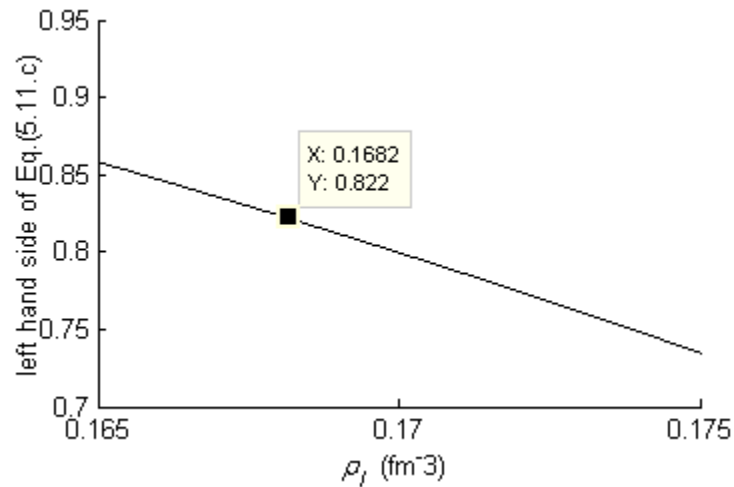


Figure 5.5 shows the left hand side of Eq. (5.11.c) as a function of the liquid density.

From Figure 5.5 we find the value of the left hand side at the equilibrium density which is 0.822. From Eq. (5.11.c) this value also equals $\mu_1(T, \rho_v, \alpha_v)$ at the equilibrium point and can be used to determine α_v as in the next step.

Finally: plot $\mu_1(T, \rho_v, \alpha_v)$ as a function of α_v at the vapor density calculated at the equilibrium point. This is shown in Figure 5.6. Then we get $\alpha_v = 0.0515$ which is a small value of the asymmetry parameter.

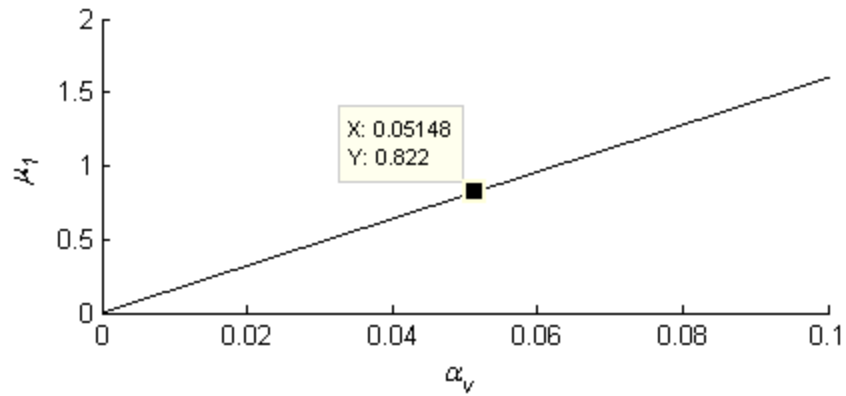


Figure 5.6 shows $\mu_1(T, \rho_v, \alpha_v)$ plotted against α_v .

We see that the vapor asymmetry parameter is small. This is why we can neglect the asymmetry corrections added to the vapor as we mentioned earlier in this chapter. Table 6 summarizes the values of the limiting temperatures and the asymmetry parameter that were obtained for the nuclei $^{109}_{47}\text{Ag}$ and $^{208}_{92}\text{Pb}$ for different Skyrme parameterizations. These values were obtained following the same steps above. The limiting temperatures obtained in our work when neglecting the vapor asymmetry corrections are the same as that obtained previously in [5].

Nucleus	σ	Without clusters (This Work)			
		T_l (MeV)	ρ_l (fm^{-3})	ρ_v (fm^{-3})	α_v
^{208}Pb	1	7.60	0.1652	0.0137	0.1500
^{208}Pb	0.25	5.49	0.1689	0.0077	0.1700
^{109}Ag	1	9.22	0.1642	0.0168	0.0522
^{109}Ag	0.25	6.80	0.1682	0.0100	0.0515

Table 6: The values of the limiting temperature, the liquid and the vapor densities and the vapor asymmetry parameter obtained at the limiting temperature. These values were obtained by neglecting the asymmetry corrections for the vapor in Eqs (5.11.a) and (5.11.b).

Now let us solve the coexistence equations, Eqs. (5.11) exactly, in this case the asymmetry corrections are added to both the drop and vapor sides of Eqs. (5.11.a) and (5.11.b). We begin the calculations by substituting the liquid equilibrium density obtained in Table 6 in the left hand side of Eq. (5.11.c), and then we calculate the vapor asymmetry parameter α_v at each value of vapor density ρ_v :

$$\alpha_v = \frac{\mu_1(T, \rho_l, \alpha_l) - \frac{1}{2} \mu_{Coul}(\rho_l)}{\left\{ \frac{4}{3} \left(x_0 + \frac{1}{2} \right) a_0 \rho_v - 2a_3 \rho_v^{1+\sigma} + T \left[1 + \sum_{n=1}^{\infty} n b_n \left[\frac{\lambda_T^3 \rho_v}{2g} \right]^n \right] \right\}}$$

where $g=2$.

The value of α_v is then used in the right hand side of Eqs. (5.11.a) and (5.11.b) and so, these equations are solved for the limiting temperature and the asymmetry parameter α_v . The calculation is repeated until self-consistency is achieved. In practice one iteration is found to be sufficient. The values of the limiting temperatures and other parameters obtained in this way are summarized in Table 7 below for different nuclei. The values of the limiting temperature obtained in this case are the same as that obtained in [5].

Nucleus	σ	Without clusters (This Work)			
		T_l (MeV)	ρ_l (fm ⁻³)	ρ_v (fm ⁻³)	α_v
²⁰⁸ Pb	1	7.48	0.1656	0.0137	0.1500
²⁰⁸ Pb	0.25	5.47	0.1685	0.0079	0.1691
¹⁰⁹ Ag	1	9.20	0.1643	0.0169	0.0519
¹⁰⁹ Ag	0.25	6.80	0.1690	0.0102	0.0504

Table 7: The values of the limiting temperatures, densities, and the vapor asymmetry parameters obtained when the coexistence equations are solved exactly.

It is seen that the values of the asymmetry parameter are larger for the lead nucleus than that for the silver nucleus. Larger values of α_v mean a larger percentage of neutrons are in the vapor. This difference may be attributed to the larger number of protons in the lead nucleus. This increases the potential barrier that the protons inside the nucleus face and prevents them from evaporation.

Comparing the results summarized in Table 6 and Table 7 it is seen that solving for the vapor asymmetry parameter exactly does not change drastically the results of the limiting temperatures, this can be understood when comparing the results of the limiting temperatures, vapor and liquid densities, and the vapor asymmetry parameters calculated in the two cases when including the vapor asymmetry corrections and when neglecting them, for example we look at the results of the ^{109}Ag nucleus at the Skyrme parameterization $\sigma=1$ the limiting temperature that is calculated in the two cases differ only by 0.02 MeV, also very small differences are noticed when comparing the values of the liquid and vapor densities and the vapor asymmetry parameters obtained in the two cases.

CHAPTER 6. RESULTS AND CONCLUSIONS

In this chapter we study the effect of the presence of clusters in the surrounding vapor on the stability of hot nuclei. Including clusters in the vapor is the main significant difference between this study and that reported in [5]. We will compare the results of this work mainly with those of [5].

6.1. THE COEXISTENCE EQUATIONS WITH CLUSTERS IN THE VAPOR

We will assume that the vapor surrounding the hot nucleus is an infinite uniform distribution of clustered nuclear matter at low density, composed of nucleons, tritons, helions, deuterons, and alphas, all assumed to be uncharged. We have derived the equation of state that describes this clustered vapor in chapter (4) using the nuclear statistical equilibrium model.

The nuclei that are immersed in the vapor are treated as hot liquid drops, they are assumed to exist in thermal, mechanical, and chemical equilibrium with the surrounding vapor. Mechanical equilibrium requires the equality of the pressure inside and outside the hot nucleus. Chemical equilibrium requires the equality of the chemical potential of protons inside and outside the hot nucleus and similarly for the chemical potential of the neutrons. Here it must be noted that chemical equilibrium is already attained between the clusters and the nucleons in the vapor by the use of the NSE model. These conditions of equilibrium are essentially the same as the coexistence equations (5.9). The only modification is the inclusion of the effect of the clusters in the vapor pressure. Here these coexistence conditions are written as:

$$\begin{aligned} \tilde{P}(T, \rho_l) + P_{sym}(T, \rho_l, \alpha_l) + P_{Coul}(\rho_l) + P_{surf}(T, \rho_l) & \quad (6.1.a) \\ & = P_{free}(T, \rho_v) + P_{clus}(T, \rho_v) + P_{sym}(T, \rho_{free}, \alpha_v) \end{aligned}$$

$$\tilde{\mu}(T, \rho_l) + \mu_{n,sym}(T, \rho_l, \alpha_l) = \mu_{free}(T, \rho_{free}) + \mu_{n,sym}(T, \rho_{free}, \alpha_v) \quad (6.1.b)$$

$$\begin{aligned} \tilde{\mu}(T, \rho_l) + \mu_{p,sym}(T, \rho_l, \alpha_l) + \mu_{Coul}(\rho_l) & \quad (6.1.c) \\ & = \mu_{free}(T, \rho_{free}) + \mu_{p,sym}(T, \rho_{free}, \alpha_v) \end{aligned}$$

Where the subscript “free” refers to the contributions of the free nucleons in the vapor, and it is calculated by the use of the ideal gas equation of state given by Eq. (2.26).

$\tilde{P}(T, \rho)$: is the pressure of symmetric nuclear matter with the Skyrme interaction given by Eq.(3.30).

$P_{clus}(T, \rho_v)$ is the pressure of the clusters in the vapor and contains contributions from all the clusters.

P_{sym} is the pressure term that results from the asymmetry of the nuclear matter derived previously in chapter (3), and it is given by Eq. (3.31).

$P_{Coul}(\rho_l)$ and $P_{surf}(T, \rho_l)$ are the Coulomb and surface terms of the pressure inside the hot liquid drop . They are given by Eqs. (5.4) and (5.7) respectively.

$\tilde{\mu}(T, \rho)$ is the chemical potential of symmetric nuclear matter with the Skyrme interaction given by Eq. (3.22).

$\mu_{n,sym}$ and $\mu_{p,sym}$ are the chemical potential terms resulting from the asymmetry of the nuclear matter for the protons and neutrons, respectively. They are given by Eq. (3.23) and (3.27).

In calculating the limiting temperature for this case we follow the procedure of chapter (5). We can write the coexistence equations (6.1) in analogy with Eqs. (5.11) as:

$$\tilde{P}(T, \rho_l) + P_{sym}(T, \rho_l, \alpha_l) + P_{Coul}(\rho_l) + P_{surf}(T, \rho_l) \quad (6.2.a)$$

$$= P_{free}(T, \rho_v) + P_{clusters}(T, \rho_v) + P_{sym}(T, \rho_{free}, \alpha_v)$$

$$\tilde{\mu}(T, \rho_l) + \mu_2(T, \rho_l, \alpha_l) + \frac{1}{2}\mu_{Coul}(\rho_l) = \mu_{free}(T, \rho_{free}) + \mu_2(T, \rho_{free}, \alpha_v) \quad (6.2.b)$$

$$\mu_1(T, \rho_l, \alpha_l) - \frac{1}{2}\mu_{Coul}(\rho_l) = \mu_1(T, \rho_{free}, \alpha_v) \quad (6.2.c)$$

where μ_1 and μ_2 are given by Eqs. (3.24) and (3.25) in chapter (3). The quantities μ_1 and μ_2 on the right-hand side of Eqs. (6.2.b) and (6.2.c) give the contribution of the chemical potential of the free nucleons in the vapor. In the NSE model the only interaction between nucleons in the vapor is by forming clusters. The Skyrme interaction parameters a_0 and a_3 in Eqs. (3.24), (3.25) and (3.31) are therefore set to zero on the right-hand side of Eqs. (6.2.a), (6.2 b), and (6.2.c).

6.2. THE LIMITING TEMPERATURE

In our calculations we will take into account the asymmetry terms added to the drop equations only. We will find that the density of free nucleons in the vapor is very small and most of the contribution to the vapor pressure comes from the clusters. We thus neglect the asymmetry terms on the right hand side of Eqs. (6.2.a) and (6.2.b) which thus become decoupled of Eq. (6.2.c). Then we solve the two Eqs. (6.2.a) and (6.2.b) for the equilibrium values and we use equation (6.2.c) to get the vapor asymmetry parameter α_v at any temperature T.

A plot of the pressure versus chemical potential is shown in Figure 6.1 at $T=2.8\text{MeV}$ and for the $\sigma=0.25$ Skyrme interaction for the nucleus $^{109}_{47}\text{Ag}$ immersed in a clustered nuclear vapor. We see that the pressure reaches a maximum value then drops indicating that the system enters the mechanically unstable region beyond the maximum, while the chemical potential keeps steadily increasing. In Figure 5.3 the pressure and chemical potential both reach the maximum value at the same time and then they fall side by side. The difference between the two Figures is a result of including clusters in the calculations represented in Figure 6.1.

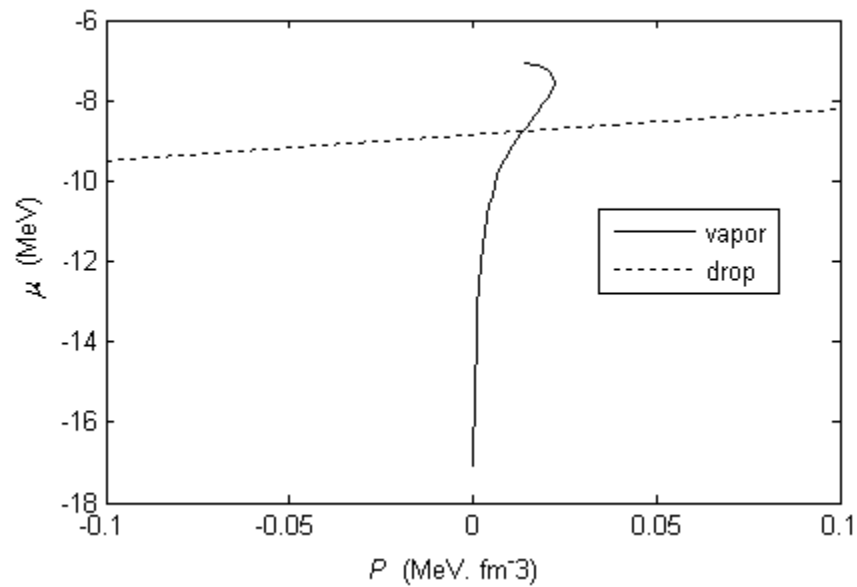


Figure 6.1: shows the chemical potential versus pressure for a ^{109}Ag nucleus at $T=2.8\text{ MeV}$ in the presence of clusters in the vapor state. The dotted line shows the chemical potential of the liquid drop (LHS of Eq. (6.2.b)) versus the corresponding pressure (LHS of Eq. (6.2.a)). The continuous line shows the same quantities for the vapor state.

From Figure 6.1 the equilibrium point has the values: $P = 0.01392\text{ MeV.fm}^{-3}$ and $\mu = -8.759\text{ MeV}$ and it occurs in the mechanically-stable region. The Figure therefore

shows that $T=2.8\text{MeV}$ is below the limiting temperature and that the limiting temperature has a higher value.

In Figure 6.2 we are calculating the limiting temperature of the silver nucleus $^{109}_{47}\text{Ag}$ using the Skyrme interaction with $\sigma=0.25$. The Figure shows that the limiting temperature for this nucleus is $T=3.3\text{ MeV}$. We see that at the limiting temperature the drop curve intersects the vapor curve at the maximum pressure. At temperatures above the limiting temperature the intersection will take place in the mechanically unstable region and the drop will fragment into parts.

We calculated the values of the limiting temperatures for the nuclei $^{109}_{47}\text{Ag}$ and $^{208}_{82}\text{Pb}$ using the Skyrme parameterizations with $\sigma = 1$ and $\sigma = 0.25$. The results are summarized in Table 8 where we also show the results obtained earlier in Chapter (5) without the inclusion of clusters in the surrounding vapor.

Nucleus	Σ	Without clusters				With clusters				
		T_L	ρ_l	ρ_v	α_v	T_L	ρ_l	ρ_v	α_v	ρ_{free}
^{208}Pb	1	7.6	0.1652	0.01370	0.15000	2.8	0.153	0.0376	0.599	0.0003
^{208}Pb	0.25	5.49	0.1689	0.00772	0.17000	2.8	0.172	0.0376	0.545	0.0003
^{109}Ag	1	9.22	0.1642	0.01678	0.05220	3.3	0.169	0.0405	0.187	0.00035
^{109}Ag	0.25	6.8	0.1682	0.01000	0.05147	3.3	0.170	0.0405	0.190	0.00035

Table 8: Comparison between the results with and without clusters included in the vapor. T_L is the limiting temperature (in MeV), ρ_l and ρ_v are the equilibrium liquid and vapor densities (in fm^{-3}) and α_v is the vapor asymmetry parameter, ρ_{free} is the density of free nucleons (in fm^{-3}) in the vapor, all evaluated at the limiting temperatures when the vapor asymmetry parameters are neglected.

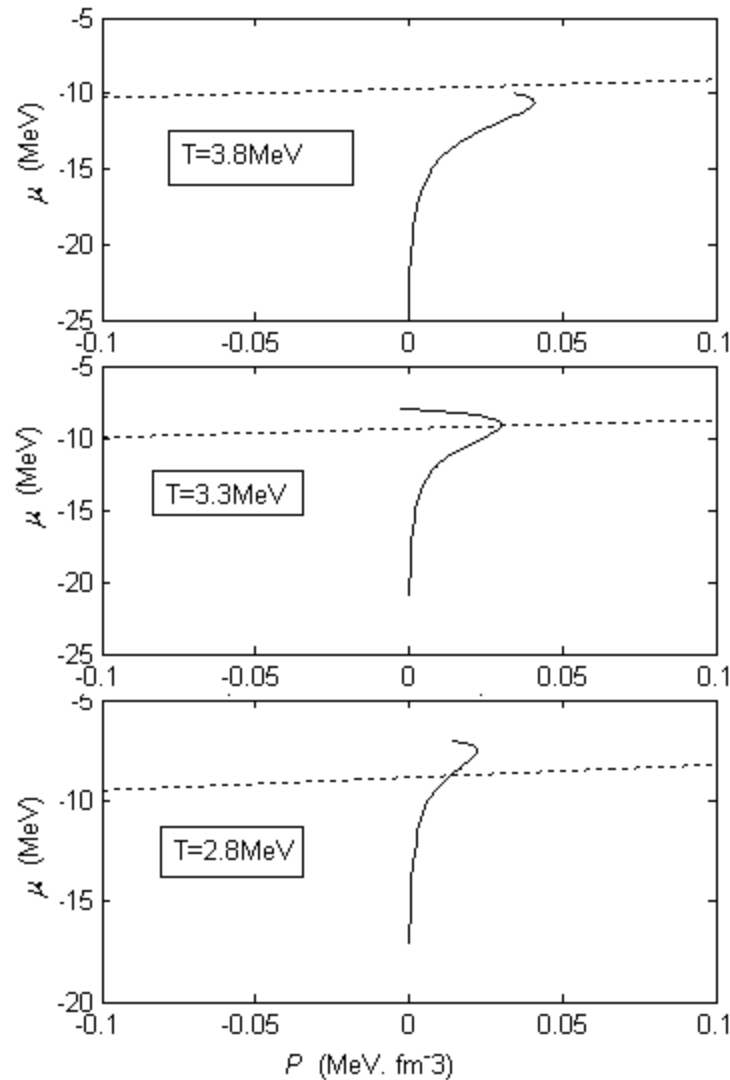


Figure 6.2: Determining the limiting temperature for a hot ^{109}Ag nucleus in the presence of clusters in the vapor state. The dotted line shows the chemical potential of the liquid drop (LHS of Eq. (6.2.b)) versus the corresponding pressure (LHS of Eq. (6.2.a)). The continuous line shows the same quantities for the vapor state.

We see in Table 8 that the free nucleon density is very small compared with the total vapor density calculated at the limiting temperature. This indicates that the vapor consists mainly of clusters, and justifies neglecting α_v (the asymmetry of the free nucleons) in solving the coexistence equations. Here it must be emphasized that α_v is the asymmetry of the free nucleons only. The total asymmetry of the vapor is much less and

close to zero, we evaluated the value of this parameter to be of order 10^{-6} at the temperatures 2.8 and 3.3 MeV, and of order 10^{-5} at $T=8\text{MeV}$. These values are reasonable since the vapor consists essentially of symmetric clusters and not free nucleons.

6.3. Conclusions

We can conclude from Table 8 the following:

- a) Including clusters in the vapor state lowers the value of the limiting temperature in comparison with that obtained in [5] where the clusters were not taken into account.
- b) For a certain nucleus (e.g. $^{109}_{47}\text{Ag}$) the value of the limiting temperature obtained with the $\sigma=0.25$ Skyrme interaction is the same as that obtained with the $\sigma=1$ Skyrme interaction. This result is not surprising because the Skyrme interaction does not play any role in the NSE model and the vapor constituents are assumed to be non-interacting aside from the condition of chemical equilibrium.
- c) The limiting temperature for the $^{208}_{82}\text{Pb}$ nucleus is smaller than the limiting temperature of the $^{109}_{47}\text{Ag}$ nucleus. This is expected since the Coulomb instability is a result of the Coulomb force acting between protons in the nucleus. Since the $^{208}_{82}\text{Pb}$ nucleus has a larger number of protons than the $^{109}_{47}\text{Ag}$ nucleus, the effect of the Coulomb force is larger and the limiting temperature will be lower for $^{208}_{82}\text{Pb}$. The result that the limiting temperature is lower for nuclei with larger number A (and hence larger number Z) was also obtained in References [3, 5].

In this thesis we include only light clusters (deuterons, helions, tritons, and alphas) while other heavier clusters may be formed in the low density nuclear matter. In a future work these heavier clusters may be included and their effect on the limiting temperature may be investigated.

Medium modifications such as the density dependent effective masses of nucleons and clusters are not included. Future work may include medium effects and give more realistic results.

The effect of the charge of the vapor and the density dependent effective mass has been investigated by Jaqaman in [7] but is neglected in the present work.

This work can be used to study supernovae explosions, and examine the early evolution of the universe. In such systems we have hot nuclei immersed in a hot surrounding vapor. The stability of these hot nuclei will play a role in determining the changing behavior of the system with time.

REFERENCES

- [1] Jaqaman. H. R, Mekjian. A. Z and L. Zamick. 1984. Liquid gas phase transitions in finite nuclear matter. *Physical Review C* 29 (6): 2067-2074.
- [2] Jaqaman. H. R, Mekjian. A. Z and L. Zamick. 1983. Nuclear Condensation. *Physical Review C* 27 (6): 2782 – 2793.
- [3] Levit. S, and P. Bonche. 1985. Coulomb instability in hot compound nuclei approaching liquid gas transition. *Nuclear Physics A* 437:426-442.
- [4] Song. H. Q and R. K. Su. 1991. Coulomb instability in hot nuclei with Skyrme interaction. *Physical Review C* 44 (6):2505-2511.
- [5] Jaqaman. H. R. 1989. Coulomb instability of hot nuclei. *Physical Review C* 39 (1): 169-176.
- [6] Song. H. Q, Qian. Z. X. and R.K. Su. 1993. Coulomb instability of hot nuclei in quantum hadrodynamics. *Physical Review C* (5): 2001-2007.
- [7] Jaqaman. H. R. 1989. Instability of hot nuclei. *Physical Review C* 40 (4): 1677-1684.
- [8] Song. H. Q, Qian. Z. X. and R.K. Su. 1994. Coulomb instability of hot nuclei with derivative scalar coupling. *Physical Review C* 49 (6):2924-2931.
- [9] Horowitz. C. J and A. Schwenck. 2006. Cluster formation and the virial equation of state of low density nuclear matter. *Nuclear Physics A* 776: 55-79.
- [10] Typel. S, Röpke. G, Klähn. K, Blaschke. D, and H. Walter. 2010. Composition and Thermodynamics of nuclear matter with light clusters. *Physical Review C* 81: 1-22.
- [11] Röpke. G. 2010. Medium effects and quantum condensates in low density nuclear matter. *Acta Physica Polonica B* 3 (3) 649-685.
- [12] Röpke. G, Grigo. A, Sumiyoshi. K and H. Shen. 2005. The nuclear matter equation of state including light clusters. *PEPAN letters* 128 (5): 25-36.
- [13] Beyer. M, Strauss. S, Schuck. P and S. A. Sofianos. 2004. Light clusters in nuclear matter of finite temperature. *European Physical Journal EPJ* 22 (2): 261-269.
- [14] Vautherin. D and D. M. Brink. 1972. Hartree-Fock calculations with Skyrme's interactions. I. Spherical nuclei. *Physical Review C* 5 (3):626-647.
- [15] Skyrme. T. (1959). The effective nuclear potential. *Nuclear Physic* 9(4):615-634.
- [16] Wong. S. 2004. *Introductory Nuclear Physics*. Weinheim: WILEY-VCH Verlag GmbH&Co. KGaA.

- [17] Horowitz. C. J and A. Schwenck . 2006. The neutrino response of low density neutron matter from the virial expansion. *Physics letters B* 642: 326-332.
- [18] Mekjian. A. Z 1978. Explosive nucleosynthesis, equilibrium thermodynamics and relativistic heavy ion collisions. *Physical Review C*. 17 (3):1051-1070.
- [19] Clifford. F. E, and Tayler. R. J. the equilibrium distribution of nuclides in matter at high temperatures. *Memoirs of the royal astronomical society*. 69 : 21- 70.
- [20] Audi. G, Wapstra. A and C. Thibault. 2003. The AME 2003 Atomic mass evaluation. *Nuclear Physics A* 729: 337-776.
- [21] Goodman Alan. L, Kapusta. Joseph. I, and Mekjian Aram. Z, 1984, liquid- gas phase instabilities and droplet formation in nuclear reactions. *Physical Review C* 30 (3): 851-866.
- [22] MATLAB version 7.10.0. Natick, Massachusetts: The MathWorks Inc., 2010.

APPENDIX A

Series Reversion:

Given the series $Y = \sum_i c_i x^i = c_1 x + c_2 x^2 + c_3 x^3 + \dots$ we can reverse this series and write:

$$x = \sum_i A_i Y^i = A_1 Y + A_2 Y^2 + A_3 Y^3 + \dots$$

Substitute $x = A_1 Y + A_2 Y^2 + A_3 Y^3 + \dots$ in the power series of Y, then by the equality of the two sides the coefficients of the new inverted series are found:

$$A_1 = \frac{1}{c_1} \tag{A.1}$$

$$A_2 = -c_1^{-3} c_2$$

$$A_3 = c_1^{-5} (2c_2^2 - c_1 c_3)$$

$$A_4 = c_1^{-7} (5c_1 c_2 c_3 - c_1^2 c_4 - 5c_2^3)$$

$$A_5 = c_1^{-9} (6c_1^2 c_2 c_4 + 3c_1^2 c_3^2 + 14c_2^4 - c_1^3 c_5 - 21c_1 c_2^2 c_3)$$

$$A_6 = c_1^{-11} (7c_1^3 c_2 c_5 + 7c_1^3 c_3 c_4 + 84c_1 c_2^3 c_3 - c_1^4 c_6 - 28c_1^2 c_2 c_3^2 - 42c_2^5 - 28c_1^2 c_2^2 c_4)$$

$$A_7 = c_1^{-13} (8c_1^4 c_2 c_6 + 8c_1^4 c_3 c_5 + 4c_1^4 c_4^2 + 120c_1^2 c_2^3 c_4 + 180c_1^2 c_2^2 c_3^2 + 132c_2^6 - c_1^5 c_7 - 36c_1^3 c_2^2 c_5 - 72c_1^3 c_2 c_3 c_4 - 12c_1^3 c_3^3 - 330c_1 c_2^4 c_3)$$